NATIONAL ADVISORY COMMITTEE
FOR AERONAUTICS

TECHNICAL NOTE 3589

DESIGN CRITERIA FOR AXISYMMETRIC AND TWO-DIMENSIONAL

SUPERSONIC INLETS AND EXITS

By James F. Connors and Rudolph C. Meyer

Lewis Flight Propulsion Laboratory
Cleveland, Ohio

NACA

Washington

January 1956

NATIONAL ADVISORY COMMITTEE FOR AERONAUTICS

TECHNICAL NOTE 3589

DESIGN CRITERIA FOR AXISYMMETRIC AND TWO-DIMENSIONAL

SUPERSONIC INLETS AND EXITS

By James F. Connors and Rudolph C. Meyer

SUMMARY

For Mach numbers up to 4.0, design charts are presented for single- and double-oblique-shock inlets and for isentropic axisymmetric and two-dimensional surfaces having theoretically focused Mach lines. Nondimensional geometric contours with corresponding local Mach number and flow-angle variations are presented for a systematic family of isentropic surfaces for Mach numbers from 2.0 to 4.0 in increments of 0.25. All solutions are carried from the free-stream Mach number to a local Mach number of unity and are applicable for use in the design of either inlets or exhaust nozzles.

For isentropic inlet applications, there exists a compression limit based on a theoretical analysis of shock structures having a single wave-intersection at the cowl lip and satisfying the condition of equal pressures and flow direction on either side of the vortex sheet. Shock solutions corresponding to this limit are demonstrated by the use of pressure-deflection polars. At a free-stream Mach number of 4.0, an all-external-compression inlet with focused compression at the cowl lip is thus limited to a theoretical total-pressure recovery of 0.685 determined solely by shock losses.

The requirement of both internally and externally attached shocks at the cowl lip is also considered. For isentropic inlets, this consideration is less restrictive with regard to maximum total-pressure recovery than the limit based on shock structure.

A comparison was then made of the performance of the isentropic inlet designed on the basis of the shock-structure compression limit and the theoretical optimum performance of single- and double-oblique-shock configurations for free-stream Mach numbers up to 4.0.

INTRODUCTION

Because of their high performance, isentropic surfaces having theo-
retically focused Mach lines may find extensive application either as
inlets or as exhaust nozzles on jet engines at Mach numbers of approxi-
mately 2.0 and higher. The design of such surfaces is based on the meth-
od of characteristics and, at least for the axisymmetric case, becomes
quite tedious and time-consuming. For the convenience of the designer,
the contours and flow fields for a pertinent family of two-dimensional
and axisymmetric surfaces were calculated with the aid of an electronic
computing machine (a Card-Program Calculator) at the NACA Lewis labora-
tory. The results are presented herein for a range of free-stream Mach
numbers up to 4.0.

For supersonic inlets operating at the higher Mach numbers (i.e.,
above 2.2) and having the specification of focused compression or a sin-
gle wave intersection at the cowl lip, the amount of external compression
is limited to a value equal to or lower than the corresponding free-
stream normal-shock pressure rise. This restriction is a consequence of
the requirement of a static-pressure balance across the resultant vortex
sheet. Another design condition which could impose a compression limit
upon the performance of isentropic inlets is the requirement of both ex-
ternally and internally attached shocks at the cowl lip. For free-stream
Mach numbers up to 4.0, theoretical analyses are made in order to define
these compression limits more precisely and to determine the extent to
which inlet performance would be limited. The results are presented
herein.

In order to illustrate the relative performance attainable with the
various types of compression surface, a comparison of theoretical pres-
sure recoveries was made for a zero-spillage isentropic inlet at its
compression limit and for the optimum configurations of single- and
double-oblique-shock inlets. All pressure recoveries are based solely
on shock losses with no accounting for viscous effects. Because of the
lack of an adequate theoretical solution for boundary layers in the pres-
ence of high adverse pressure gradients, no boundary-layer displacement
correction was applied to the resulting contours. Also, the external
drags associated with each type of inlet were not considered in any of
the comparisons.

SYMBOLS

The following symbols are used in this report:

A   area

M   Mach number

P   total pressure

p   static pressure

r   radius of focal point

x   axial distance from tip of spike or leading edge of ramp

y   height or radial distance from axis

γ ratio of specific heats for air

λ flow angle relative to free-stream direction, deg

λ_{d,M_0} two-dimensional detachment angle corresponding to free-stream Mach number, deg

λ_{d,M_e} two-dimensional detachment angle corresponding to the Mach number at the diffuser entrance, deg

λ_1 initial wedge angle, deg

λ_2 difference between initial and second wedge angles, deg

θ_1 initial cone half-angle, deg

θ_2 difference between initial and second cone half-angle, deg

η_{ke} kinetic-energy efficiency defined as the ratio of kinetic energy available after diffusion (assuming isentropic reexpansion to ambient pressure) to the kinetic energy in the free stream,

$$1 - \frac{2}{(\gamma - 1)M_0^2}\left[\left(\frac{P_0}{P_3}\right)^{\frac{\gamma-1}{\gamma}} - 1\right]$$

ψ ray angle, a conical half-angle that can vary between the conical shock angle and the cone half-angle

Subscripts:

a   conditions between strong shock and vortex sheet

b   conditions between vortex sheet and reflected wave

c   conditions between reflected wave and end of the isentropic compression fan

e   conditions at diffuser entrance

f   conditions at focal point

l conditions corresponding to compression limit

s   conditions along compression surface

O   free-stream conditions

1   conditions behind initial shock

3   conditions behind normal shock (after supersonic compression has
           been completed)

ANALYSIS AND DISCUSSION

The assumptions and calculation procedure used in the design of
isentropic surfaces are considered first. Important geometric and aero-
dynamic parameters are summarized in chart form. Then, an analysis of
compression limits pertaining to supersonic inlets is presented. Finally,
a comparison of theoretical pressure recoveries is made of the various
types of inlet for free-stream Mach numbers up to 4.0 when these compres-
sion limits are imposed.

Design of Isentropic Surfaces

The following design conditions were imposed in order to establish
and define a systematic family of isentropic surfaces, such as would be
suitable for supersonic inlet (or exit) applications:

(1) The total-pressure recovery across the initial shock is 0.99

(2) All characteristic lines coalesce or focus at a common inter-
     section

(3) Zero-radius turning (Prandtl-Meyer flow) occurs at the focal
     point which is located on the initial shock

A calculation was made to determine the effect of initial shock
strength on over-all pressure recovery for a specified amount of flow
turning, that is, the balance between normal- and oblique-shock losses.
The question was whether it is more desirable to utilize a completely
isentropic compression before the normal shock or, for the same degree
of flow turning, to have a finite initial shock followed by isentropic
compression and a normal shock at a correspondingly lower Mach number.

The computation was based on an assumed cowl, which had an initial ex-
ternal angle equal to the free-stream detachment value and the internal
surface alined with the local flow. The results of this analysis indi-
cated that, for a specified turning, completely isentropic compression
ahead of the normal shock ($P_1/P_0 = 1.00$) offers the maximum potential re-
covery for all-external-compression inlets. In practice, however, it is
generally desirable to have a finite initial compression surface angle in
order to avoid overly thin, long surfaces. Accordingly, the total-
pressure recovery across the initial shock P_1/P_0 was arbitrarily set at
0.99 for the present family of isentropic surfaces without much loss in
over-all recovery (the associated decrement in P_3/P_0 for the preceding
computation was a maximum of 0.01 at a free-stream Mach number of 2.0 and
0.005 at a free-stream Mach number of 4.0). This results in a variation
in the initial compression surface angle with free-stream Mach number,
the larger angles occurring in the lower speed range.

A typical axisymmetric spike calculation is graphically illustrated
in figure 1. For a particular Mach number, the first design condition
of a total-pressure recovery across the tip shock of 0.99 established
both the initial cone and its shock angle. These values were determined
by means of the conical-shock charts of reference 1. The initial charac-
teristics line was then determined from the conical flow field (ref. 2).
At the focal point, two-dimensional reverse-Prandtl-Meyer-streamline re-
lations held with zero turning radius. From these two sets of data, the
isentropic flow field was calculated by the method of characteristics
for potential flow with axial symmetry (ref. 3). Iterations based on the
procedure of reference 4 were used in the computation of each point in
the characteristics network. By means of a stream-function integration
along each of the focused characteristics (ref. 5), the surface contour
was determined from continuity relations. The end point ($M = 1.00$) was
also calculated from the continuity equation with the additional assump-
tions of a straight sonic line and one-dimensional flow.

Axisymmetric spike solutions were thus computed for Mach numbers
from 2.0 to 4.0 in increments of 0.5. The calculated results are given
in table I. An interpolation was made in order to determine the neces-
sary data for the 0.25 Mach number increments. All the results are sum-
marized in figure 2. Dimensionless geometric contours with their corres-
ponding focal points are presented in figure 2(a). For each value of
axial distance x/r, the local surface angle and Mach number are given
in figure 2(b). Conditions at the focal point corresponding to a surface
point x/r obtained by tracing back along a characteristic line may be
obtained from figure 2(c). Thus, all the pertinent information necessary
in the design of isentropic axisymmetric centerbodies and the condition
of the flow in the vicinity of the cowl lip may now be determined from
the appropriate charts.

A parallel presentation of similar design parameters for two-
dimensional isentropic ramps is given in figure 3. Design conditions
identical to those for the axisymmetric cases were imposed. Geometric
contours and corresponding focal points are presented in figure 3(a).
In the two-dimensional case, the flow conditions along any characteris-
tic line are, of course, constant. Thus, the conditions at the surface
are the same as those at the focal point. The variation of Mach number
and flow angle with axial distance x/r are presented in figure 3(b).
In the two-dimensional case, the calculation of isentropic contours and
flow fields with focused characteristics simply involves the use of the
Prandtl-Meyer theory for flow around corners. A convenient tabulation
and definition of the particular parameters are presented in table II.
With the use of these relations, the contours and flow fields correspond-
ing to any other choice of initial shock strength may be readily
determined.

In a comparison of figures 2(c) and 3(b), there was a slight dis-
crepancy in the initial values of local Mach number and flow angle in-
stead of the expected correspondence. This was incurred in the axisym-
metric cases through the use of the conical-shock charts of reference 1.
Some of the variation can be attributed to a difference in the ratio of
specific heats for air γ and some to chart accuracy. This discrepancy
amounts to less than 1° in flow deflection through the initial shock.
The net effect is believed to be negligibly small with regard to either
inlet or exit designs.

The charts of figures 2 and 3 may be used for the design of isen-
tropic exit plugs or exhaust nozzles with only negligibly small error in
thrust because of the initial conical flow assumed in the present calcu-
lations. The ratios of the theoretical thrust corresponding to these
contours to the ideal thrust were computed and found to be on the order
of 0.5 percent less than unity. In the axisymmetric designs, the error
in centerbody surface angle at the throat would be a maximum of 0.1°.
These errors are deemed small enough to make the charts equally appli-
cable to exit-design problems.

Compression Limits for Isentropic Inlets

An analysis was made to determine the theoretical limitations upon
the performance (i.e., total-pressure recovery) of supersonic isentropic
inlets. The following two conditions for inlets having focused compres-
sion at the cowl-lip were investigated: (1) maximum recovery based on
shock-structure requirements of pressure and flow direction, and (2)
maximum recovery based on shock attachment at the cowl lip, both intern-
ally and externally.

3659

As illustrated in figure 4, the branch-shock configuration to be analyzed consists of a single intersection of an isentropic compression fan, possibly a reflected wave (either an expansion or a compression), a vortex sheet, and a shock wave. Theoretical requirements of any wave intersection are that equal static pressures and flow direction must exist on either side of the vortex sheet. Two-dimensional flow relations are used in the present analysis; however, the results are equally applicable to the axisymmetric case since the flow at the focal point can also be considered as locally two dimensional. Theoretical solutions are demonstrated by means of pressure-deflection polars as described, for example, in reference 6. In figure 5, free-stream shock polars are represented by the solid curves, while the pressure-deflection characteristics of the isentropic compression fields, or isentropes, are identified by the short dashed lines.

In order to satisfy the condition of equal pressures and flow direction across the vortex sheet, a theoretical solution requires an intersection of the reflected-wave polar (whether it is a compression or an expansion) with the free-stream shock polar. The limiting condition occurs at a point on the isentrope corresponding to the maximum deflection angle from which a reflected-wave polar will be just tangent to the free-stream polar. This maximum isentropic compressive turning is indicated by the circular symbol on the isentrope for each Mach number. For isentropic deflection angles in excess of this limit, no theoretical solution is possible for a single intersection point of the multiwave pattern. At a Mach number of 3.5, the isentropic turning limit occurs at the intersection of the isentrope and the free-stream shock polar (no reflected wave being required). At Mach numbers greater than 3.5, a weak expansion is required as a reflected wave, whereas at the lower Mach numbers the reflected waves are compressions. At a Mach number of 1.5, the isentrope is almost coincident with and terminates on the free-stream shock polar. For Mach numbers of 2.0 and above, the over-all pressure rise at the compression limit $(p_a/p_0)_l$ exceeds by a small amount that at the maximum shock deflection angle and is considerably less (approximately 10 to 15 percent) than the free-stream normal-shock pressure rise.

The results of this analysis of the shock-structure limit are summarized in figure 6. The variation of local Mach number and turning angle corresponding to this compression limit are shown for free-stream Mach numbers up to 4.0. In addition, the theoretical maximum total-pressure recoveries (for inlets with entrance Mach numbers equal to the Mach number after the isentropic compression and ahead of the reflected wave) are likewise presented as a function of free-stream Mach number. As an example of the significance of this compression limit, at Mach number 4.0 an isentropic all-external-compression inlet with full mass flow has a theoretical maximum recovery of only 0.685 determined solely by shock losses. In this case, the local normal-shock Mach number is

2.08. Since in this analysis, the flow is considered as a two-dimensional problem, it is necessary to refer to figure 2 in order to find the equivalent limiting parameters $(\lambda_{s,\zeta}$ and $M_{s,\zeta})$ for the axisymmetric isentropic spikes. The procedure at any free-stream Mach number is as follows: Enter figure 6 to determine λ_ζ or M_ζ. With $\lambda_\zeta = \lambda_p$ or with $M_\zeta = M_p$, enter figure 2(c) and determine the corresponding value of x/r. Then, from figure 2(b) the values of $\lambda_{s,\zeta}$ and $M_{s,\zeta}$ at the compression limit may be obtained.

The requirement of attached shocks, externally and internally, at the cowl lip has also been analyzed in order to ascertain its effect upon the performance of isentropic inlets. With the cowl assumed to have a 3° included angle, performance was calculated for an isentropic inlet with an initial external cowl-lip angle equal to the free-stream detachment angle and with a local diffuser-entrance Mach number such that the internal cowl-lip angle would equal the detachment value. The results are shown in figure 7. This consideration is much less restrictive with regard to inlet performance (i.e., pressure recovery) than the compression limit based on shock structure. At Mach 4.0, this cowl-shock-attachment consideration limits the pressure recovery of isentropic inlets with no internal contraction to approximately 0.89 as compared with a value of 0.685 for the pressure recovery based on shock-structure considerations. The compression limits with the maximum allowable internal contraction for starting are also included.

In the design of high-Mach-number all-external-compression isentropic inlets having focused characteristics at the cowl lip, the compression limit based on shock structure should, in practice, receive first consideration. With flow turning in excess of this limit, it has been observed experimentally, with just a compression surface (no cowl), that a local bow shock forms and is located upstream of the design focal point. For the complete inlet this, of course, results in spillage losses (i.e., additive drags) which tend to offset any gains in recovery. Techniques for circumventing this limit, such as employing a cowl to separate the inner and outer flows, are subject to starting difficulties and viscous effects on the internal cowl surface. If such a technique were possible, the upper limit based on cowl-shock-attachment would hold.

Comparison of Optimum Performance for Various Inlet Configurations

A performance comparison was made between the isentropic inlet with its compression limit based on shock structure and several other inlet types. As mentioned previously, in this comparison only the potential internal-flow performance of the various inlets is considered. No accounting is made of the associated external drags. The results are presented in figure 8 for supersonic Mach numbers up to 4.0. In the

3659

order of increasing pressure recovery, the inlet configurations considered were normal-shock, convergent-divergent, single-cone, double-cone, and isentropic. The single-cone, double-cone, and isentropic inlets were evaluated with and without internal contraction. The geometric angles of the single- and double-cone inlets were optimized in terms of pressure recovery. As indicated by the curves, the use of the higher compression inlets becomes increasingly more desirable in terms of relative internal performance with increasing free-stream Mach number. This is also illustrated by the superimposed lines of constant kinetic-energy efficiency η_{ke}, which for the ram-jet engine is a measure of thrust performance if the combustion factors are held constant. Whereas the single-cone (no internal contraction) inlet indicates a kinetic-energy efficiency of 0.97 at a Mach number of 2.0, the isentropic inlet is required in order to yield the same internal-performance potential at a Mach number of 4.0. The perforated convergent-divergent diffuser (ref. 9) has not been considered herein; however, its internal performance does not appear to encounter any compression limitations.

Theoretical design calculations for determining optimum and off-design performance of single-oblique and double-oblique-shock inlets are presented in appendixes A and B, respectively. Both cases, the two dimensional and the axisymmetric, are considered therein.

SUMMARY OF RESULTS

Convenient charts have been presented for the design of isentropic inlets or exits, including geometric contours and local Mach number and flow-angle distributions along the surfaces and at the focal point. Limitations on the amount of compressive flow turning, that can be utilized with isentropic inlets, have been analyzed and evaluated for Mach numbers up to 4.0. A compression limit based on shock-structure requirements comes into effect at Mach number 1.5 for isentropic inlets. At Mach number 4.0, an all-external-compression isentropic inlet with a mass-flow ratio of unity is thus limited to a theoretical pressure recovery of 0.685. A comparison of optimum performance is made for several types of conventional inlets over a wide range of supersonic Mach number to illustrate the relative capability of the isentropic inlet with its compression limitation.

Lewis Flight Propulsion Laboratory
   National Advisory Committee for Aeronautics
      Cleveland, Ohio, October 21, 1955

APPENDIX A

ESTIMATED PERFORMANCE OF SINGLE-OBLIQUE-SHOCK INLETS

Theoretical total-pressure recoveries for single-cone and single-
wedge supersonic inlets with and without internal contraction are pre-
sented in figure 9. The losses, which were taken into account, occur
across one oblique shock and one normal shock. For the cases with in-
ternal contraction, the maximum permissible value for starting (ref. 7)
was used. For the axisymmetric inlets, the normal-shock Mach number was
assumed to be the arithmetic average of the Mach number immediately be-
hind the oblique shock and the Mach number along the conical surface.
The variation of pressure recovery with cone half-angle and wedge angle
is shown on the figures for free-stream Mach numbers up to 4.0. Super-
imposed on the curves are lines identifying the optimum cone or wedge
angle at each Mach number, the mixed-flow region $(M_S = 1.00)$ for the
axisymmetric inlets, and the shock-detachment condition for the two-
dimensional inlets. Both optimum and off-design performance may be ob-
tained for single-oblique-shock inlets from these figures.

APPENDIX B

ESTIMATED PERFORMANCE OF DOUBLE-OBLIQUE SHOCK-INLETS

Theoretical total-pressure recoveries for double-cone and double-wedge supersonic inlets with and without internal contraction are presented in figure 10. Total-pressure losses, in these cases, occur across two oblique shocks and one normal shock. For the cases with internal contraction, the maximum permissible value for starting (ref. 7) was used.

With the axisymmetric configurations, several simplifying assumptions were used in the calculations. The Mach number of the conical flow field of the initial cone was considered to be the arithmetic average of the Mach number immediately behind the tip shock and the Mach number along the first cone surface. The second oblique-shock loss was then calculated by considering that this averaged flow would undergo a two-dimensional flow deflection equal to the difference of the second and initial cone half-angles. This consideration also yielded an average diffuser entrance Mach number. In order to avoid shock-detachment conditions externally at the cowl lip, in some cases, the internal cowl surface must be inclined initially with the local flow, producing a resultant internal reflected wave. The compression through this wave is not considered in the no-internal-contraction case. With the maximum allowable internal contraction for starting, one-dimensional flow relations are assumed to hold from the entrance to the throat.

Although not necessary for the previous calculation of theoretical recoveries, an approximate method for constructing the curved second shock is generally quite satisfactory for use in locating the intersection of the first and second oblique shocks and in designing the cowl lip. The method was first proposed in reference 8. A linear variation of Mach number and flow inclination with ray angle ψ between the values just behind the initial oblique shock and the values at the first cone surface is assumed. With this flow distribution, a constant flow deflection (equal to the difference between the second and first cone half-angles) is then assumed across the second shock. With these assumptions, calculation and construction of the curved second shock is now possible in a progressive stepwise procedure starting from the cone surface.

From the charts of figure 10, the inlet performance for a large range of angle combinations and free-stream Mach number may be estimated. In figure 11 the optimum pressure recoveries and the corresponding optimum angle combinations are summarized for a range of free-stream Mach numbers up to 4.0.

3659

CS-2 back

REFERENCES

1. Moeckel, W. E., and Connors, J. F.: Charts for the Determination of Supersonic Air Flow Against Inclined Planes and Axially Symmetric Cones. NACA TN 1373, 1947.

2. Anon.: Tables of Supersonic Flow Around Cones. Dept. Elec. Eng., M.I.T., 1947.

3. Ferri, Antonio: Application of the Method of Characteristics to Supersonic Rotational Flow. NACA Rep. 841, 1946. (Supersedes NACA TN 1135.)

4. Cronvich, Lester L.: Numerical-Graphical Method of Characteristics for Axially Symmetric Isentropic Flow. Jour. Aero. Sci., vol. 15, no. 3, Mar. 1948, pp. 152-162.

5. Evvard, John C., and Maslen, Stephen H.: Three-Dimensional Supersonic Nozzles and Inlets of Arbitrary Exit Cross Section. NACA TN 2688, 1952.

6. Courant, R., and Friedrichs, K. O.: Supersonic Flow and Shock Waves. Interscience Pub., Inc., 1948.

7. Kantrowitz, Arthur, and Donaldson, Coleman DuP.: Preliminary Investigation of Supersonic Diffusers. NACA WR L-713, 1945. (Supersedes NACA ACR L5D20.)

8. Moeckel, W. E., Connors, J. F., and Schroeder, A. H.: Investigation of Shock Diffusers at Mach Number 1.85. II - Projecting Double-Shock Cones. NACA RM E6L13, 1947.

9. Evvard, John C., and Blakey, John W : The Use of Perforated Inlets for Efficient Supersonic Diffusion. NACA RM E51B10, 1951. (Supersedes NACA RM E7C26.)

3659

TABLE I. - CALCULATED ISENTROPIC SPIKE DESIGN PARAMETERS

x/r	y/r	M_s	λ_s	M_f	λ_f	x/r	y/r	M_s	λ_s	M_f	λ_f
$M_0 = 2.00$						$M_0 = 3.00$					
0.6172	0.2101	1.600	18.8	1.72	7.75	0.9614	0.2344	2.55	13.65	2.73	5.50
.6566	.2239	1.57	19.7	1.70	8.40	1.1237	.2742	2.53	14.6	2.65	7.17
.6978	.2387	1.55	20.2	1.68	8.99	1.2414	.3039	2.51	15.5	2.60	8.29
.7368	.2536	1.53	21.0	1.66	9.58	1.4463	.3648	2.42	17.8	2.50	10.6
.7746	.2684	1.52	21.6	1.64	10.2	1.6114	.4212	2.33	20.0	2.40	13.0
.8097	.2829	1.50	22.3	1.62	10.8	1.7474	.4737	2.24	22.3	2.30	15.4
.8442	.2968	1.48	23.0	1.60	11.35	1.8596	.5224	2.14	24.7	2.20	18.0
.9078	.3242	1.45	24.2	1.56	12.5	1.9518	.5668	2.05	27.2	2.10	20.6
.9667	.3516	1.41	25.5	1.52	13.7	2.0293	.6089	1.96	29.8	2.00	23.3
1.0200	.3775	1.37	26.6	1.48	14.9	2.0936	.6481	1.86	32.4	1.90	26.1
1.0701	.4034	1.34	27.8	1.44	16.1	2.1483	.6842	1.77	35.1	1.80	29.0
1.1171	.4288	1.30	29.0	1.40	17.2	2.1915	.7158	1.67	37.8	1.70	31.9
1.1714	.4598	1.25	30.4	1.35	18.7	2.2292	.7463	1.57	40.6	1.60	34.8
1.2223	.4904	1.20	31.8	1.30	20.0	2.2606	.7753	1.48	43.5	1.50	37.8
1.2714	.5219	1.15	33.3	1.25	21.4	2.2874	.8026	1.38	46.4	1.40	40.7
1.3200	.5553	1.10	34.6	1.20	22.7	2.3109	.8289	1.28	49.2	1.30	43.5
1.3720	.5920	1.04	35.2	1.15	23.8	2.3320	.8542	1.18	51.7	1.20	46.1
1.3210	.6980	1.00	35.3	1.00	26.2	2.3530	.8810	1.09	52.0	1.10	48.4
1.3319	1.0000		Focal point			2.3853	.9219	1.00	52.0	1.00	49.7
						2.2889	1.0000		Focal point		
$M_0 = 2.50$						$M_0 = 3.50$					
0.8083	0.2364	2.055	16.3	2.22	6.70	1.1427	0.2387	3.08	11.80	3.20	5.00
.9300	.2726	2.02	17.2	2.15	8.51	1.4074	.2958	3.01	13.2	3.10	6.86
1.0319	.3045	2.00	18.5	2.10	9.84	1.6407	.3537	2.93	15.0	3.00	8.75
1.1229	.3351	1.95	20.0	2.05	11.2	1.8379	.4105	2.83	16.8	2.90	10.7
1.2061	.3657	1.91	21.3	2.00	12.6	1.9965	.4617	2.74	18.7	2.80	12.8
1.2800	.3956	1.87	22.8	1.95	14.0	2.1303	.5089	2.65	20.6	2.70	14.9
1.3463	.4246	1.82	24.1	1.90	15.4	2.2373	.5505	2.56	22.8	2.60	17.1
1.4075	.4527	1.77	25.5	1.85	16.8	2.3325	.5926	2.46	24.8	2.50	19.4
1.4616	.4796	1.73	26.8	1.80	18.2	2.4098	.6300	2.37	27.0	2.40	21.7
1.5120	.5057	1.68	28.3	1.75	19.7	2.4755	.6647	2.27	29.3	2.30	24.2
1.5568	.5304	1.63	29.7	1.70	21.1	2.5300	.6963	2.18	31.7	2.20	26.8
1.5971	.5543	1.59	31.2	1.65	22.6	2.5771	.7263	2.08	34.2	2.10	29.4
1.6351	.5782	1.54	32.7	1.60	24.1	2.6163	.7548	1.98	36.8	2.00	32.1
1.6692	.6004	1.49	34.1	1.55	25.6	2.6484	.7805	1.89	39.5	1.90	34.9
1.6992	.6221	1.44	35.4	1.50	27.0	2.6753	.8026	1.79	42.2	1.80	37.8
1.7289	.6437	1.40	36.9	1.45	28.5	2.6989	.8251	1.69	45.0	1.70	40.7
1.7565	.6647	1.35	38.5	1.40	30.0	2.7197	.8458	1.59	47.7	1.60	43.7
1.7811	.6853	1.30	40.0	1.35	31.4	2.7358	.8658	1.49	50.8	1.50	46.6
1.8042	.7047	1.25	41.3	1.30	32.8	2.7497	.8832	1.39	53.7	1.40	49.5
1.8257	.7247	1.20	42.4	1.25	34.1	2.7616	.9000	1.28	56.5	1.30	52.3
1.8466	.7428	1.15	43.1	1.20	35.4	2.7721	.9168	1.18	59.0	1.20	55.0
1.8694	.7642	1.10	43.2	1.15	36.6	2.7816	.9352	1.08	59.3	1.10	57.2
1.8963	.7900	1.04	43.3	1.10	37.6	2.7984	.9616	1.00	59.5	1.00	58.51
1.9516	.8426	1.00	43.3	1.00	38.94	2.7326	1.0000		Focal point		
1.8115	1.0000		Focal point								
$M_0 = 4.00$											
1.1288	0.1889	3.62	9.50	3.70	4.20	3.0596	0.7784	2.29	35.3	2.30	31.5
1.5141	.2609	3.50	11.4	3.60	5.71	3.0911	.8026	2.19	37.7	2.20	34.1
1.7899	.3185	3.41	12.9	3.50	7.27	3.1158	.8226	2.09	40.2	2.10	36.7
2.0188	.3736	3.32	14.3	3.40	8.90	3.1368	.8416	2.00	42.8	2.00	39.4
2.2098	.4253	3.23	15.9	3.30	10.6	3.1553	.8584	1.90	45.5	1.90	42.2
2.3716	.4737	3.14	17.4	3.20	12.3	3.1703	.8732	1.80	48.0	1.80	45.1
2.5045	.5173	3.04	19.1	3.10	14.2	3.1835	.8895	1.70	50.8	1.70	48.0
2.6254	.5611	2.95	20.9	3.00	16.0	3.1937	.9042	1.60	53.5	1.60	50.9
2.7173	.5972	2.86	22.6	2.90	18.0	3.2028	.9174	1.50	56.2	1.50	53.9
2.8000	.6337	2.77	24.6	2.80	20.1	3.2095	.9295	1.40	58.8	1.40	56.8
2.8697	.6671	2.67	26.5	2.70	22.2	3.2158	.9411	1.30	61.4	1.30	59.6
2.9289	.6979	2.58	28.6	2.60	24.4	3.2211	.9511	1.20	63.5	1.20	62.2
2.9798	.7263	2.48	30.7	2.50	26.7	3.2258	.9616	1.10	65.5	1.10	64.5
3.0229	.7537	2.38	33.0	2.40	29.1	3.2340	.9805	1.00	66.2	1.00	65.8
						3.1910	1.0000		Focal point		

TABLE II. - TWO-DIMENSIONAL FLOW AROUND CORNERS

(Prandtl-Meyer Theory)
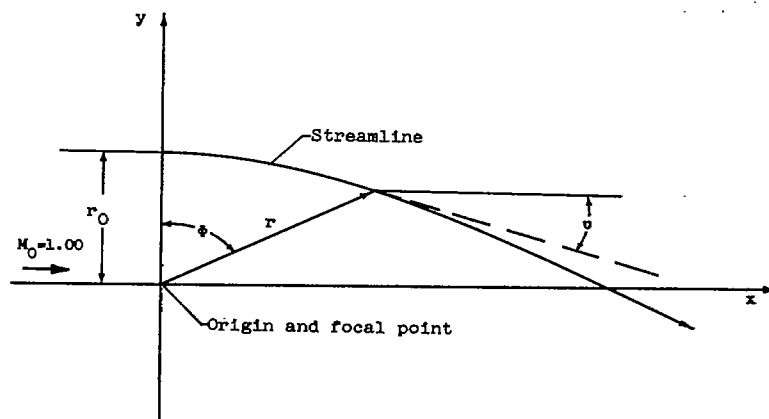
Symbols:

r, ϕ polar coordinates

x, y Cartesian coordinates

v flow angle

β Mach angle $\sin^{-1} \frac{1}{M}$

M Mach number

Equations:

$$\phi = \frac{1}{k} \tan^{-1} k\sqrt{M^2 - 1}$$

where

$$k = \sqrt{(\gamma - 1)/(\gamma + 1)}, \qquad \gamma = 1.40$$

$$v = \phi + \beta - 90 \text{ (deg)}$$

For streamlines:

$$r/r_0 = 1/(\cos k\phi)^6$$

$$x/r_0 = r/r_0 \cos(\beta - v), \qquad y/r_0 = r/r_0 \sin(\beta - v)$$

M	v	ϕ	$\dfrac{r}{r_0}$	$\dfrac{x}{r_0}$	$\dfrac{y}{r_0}$	M	v	ϕ	$\dfrac{r}{r_0}$	$\dfrac{x}{r_0}$	$\dfrac{y}{r_0}$
1.00	0.	0	1.0000	0	1.0000	1.10	1.336	25.956	1.1087	0.48526	0.99687
1.01	.04473	8.114	1.0101	.14256	.99997	1.11	1.532	27.255	1.1206	.51318	.99620
1.02	.1257	11.490	1.0203	.20325	.99989	1.12	1.735	28.501	1.1327	.54048	.99541
1.03	.2294	14.092	1.0308	.25097	.99976	1.13	1.944	29.698	1.1450	.56725	.99457
1.04	.3510	16.293	1.0414	.29215	.99953	1.14	2.160	30.854	1.1574	.59358	.99361
1.05	.4874	18.240	1.0521	.32931	.99923	1.15	2.381	31.973	1.1701	.61958	.99258
1.06	.6367	20.007	1.0631	.36370	.99890	1.16	2.607	33.057	1.1829	.64525	.99145
1.07	.7973	21.637	1.0742	.39608	.99852	1.17	2.839	34.112	1.1960	.67073	.99022
1.08	.9680	23.160	1.0856	.42695	.99807	1.18	3.074	35.138	1.2093	.69602	.98895
1.09	1.148	24.595	1.0971	.45660	.99752	1.19	3.314	36.138	1.2228	.72113	.98754
1.10	1.336	25.956	1.1087	.48526	.99687	1.20	3.558	37.115	1.2365	.74612	.98601

TABLE II. – Continued. TWO-DIMENSIONAL FLOW AROUND CORNERS

M	υ	φ	$\frac{r}{r_0}$	$\frac{x}{r_0}$	$\frac{y}{r_0}$	M	υ	φ	$\frac{r}{r_0}$	$\frac{x}{r_0}$	$\frac{y}{r_0}$
1.20	3.558	37.115	1.2365	0.74612	0.98601	1.90	23.59	81.83	2.9551	2.925	0.4199
1.21	3.806	38.071	1.2505	.77110	.98444	1.91	23.87	82.30	2.9949	2.968	.4013
1.22	4.057	39.005	1.2646	.79592	.98270	1.92	24.15	82.76	3.0349	3.011	.3824
1.23	4.312	39.921	1.2790	.82075	.98088	1.93	24.43	83.22	3.0741	3.053	.3631
1.24	4.569	40.818	1.2936	.84559	.97901	1.94	24.71	83.68	3.1143	3.095	.3429
1.25	4.830	41.700	1.3085	.87043	.97696	1.95	24.99	84.14	3.1578	3.141	.3224
1.26	5.093	42.565	1.3235	.89526	.97477	1.96	25.27	84.59	3.1990	3.185	.3016
1.27	5.359	43.416	1.3388	.91738	.97250	1.97	25.55	85.04	3.2415	3.230	.2803
1.28	5.627	44.252	1.3544	.94511	.97011	1.98	25.83	85.50	3.2873	3.277	.2579
1.29	5.898	45.075	1.3701	.97009	.96756	1.99	26.10	85.93	3.3311	3.323	.2364
1.30	6.170	45.885	1.3862	.99521	.96493	2.00	26.38	86.38	3.3750	3.368	.2131
1.31	6.445	46.678	1.4023	1.0202	.96215	2.01	26.66	86.82	3.4200	3.415	.1897
1.32	6.721	47.470	1.4190	1.0457	.95923	2.02	26.93	87.26	3.4650	3.461	.1656
1.33	7.000	48.247	1.4358	1.0712	.95615	2.03	27.20	87.69	3.5125	3.510	.1416
1.34	7.279	49.011	1.4529	1.0967	.95296	2.04	27.48	88.13	3.5613	3.560	.1162
1.35	7.561	49.766	1.4702	1.1223	.94959	2.05	27.75	88.55	3.6075	3.606	.09127
1.36	7.844	50.512	1.4879	1.1485	.94617	2.06	28.02	88.98	3.6563	3.656	.06508
1.37	8.128	51.248	1.5056	1.1742	.94246	2.07	28.29	89.40	3.7051	3.705	.03879
1.38	8.413	51.974	1.5238	1.2003	.93867	2.08	28.56	89.82	3.7552	3.755	.01179
1.39	8.699	52.692	1.5422	1.2267	.93475	2.09	28.83	90.24	3.8066	3.807	-.01595
1.40	8.987	53.402	1.5609	1.2531	.93059	2.10	29.10	90.66	3.8580	3.858	-.04444
1.41	9.276	54.105	1.5799	1.2798	.92627	2.11	29.36	91.07	3.9078	3.907	-.07296
1.42	9.565	54.798	1.5991	1.3067	.92183	2.12	29.63	91.49	3.9635	3.962	-.1031
1.43	9.855	55.484	1.6187	1.3337	.91720	2.13	29.90	91.90	4.0144	4.012	-.1331
1.44	10.15	56.17	1.6385	1.361	.9122	2.14	30.16	92.30	4.0700	4.067	-.1633
1.45	10.44	56.84	1.6589	1.389	.9074	2.15	30.43	92.71	4.1254	4.121	-.1950
1.46	10.73	57.50	1.6795	1.416	.9022	2.16	30.69	93.11	4.1806	4.174	-.2268
1.47	11.02	58.16	1.6995	1.444	.8965	2.17	30.95	93.51	4.2373	4.229	-.2594
1.48	11.32	58.81	1.7209	1.472	.8913	2.18	31.21	93.91	4.2937	4.284	-.2928
1.49	11.61	59.45	1.7425	1.501	.8857	2.19	31.47	94.30	4.3518	4.340	-.3283
1.50	11.91	60.10	1.7643	1.529	.8795	2.20	31.73	94.69	4.4092	4.395	-.3605
1.51	12.20	60.73	1.7867	1.559	.8735	2.21	31.99	95.09	4.4723	4.455	-.3988
1.52	12.49	61.35	1.8085	1.587	.8671	2.22	32.25	95.48	4.5310	4.510	-.4327
1.53	12.79	61.98	1.8312	1.617	.8603	2.23	32.51	95.87	4.5935	4.570	-.4699
1.54	13.09	62.60	1.8543	1.646	.8533	2.24	32.76	96.25	4.6555	4.628	-.5070
1.55	13.38	63.20	1.8779	1.676	.8466	2.25	33.02	96.63	4.7148	4.685	-.5446
1.56	13.68	63.81	1.9019	1.707	.8393	2.26	33.27	97.01	4.7801	4.744	-.5832
1.57	13.97	64.41	1.9260	1.737	.8318	2.27	33.53	97.39	4.8473	4.807	-.6234
1.58	14.27	65.00	1.9497	1.767	.8239	2.28	33.78	97.77	4.9116	4.866	-.6640
1.59	14.56	65.59	1.9747	1.798	.8159	2.29	34.03	98.14	4.9776	4.927	-.7048
1.60	14.86	66.18	2.0000	1.830	.8078	2.30	34.28	98.51	5.0454	4.990	-.7467
1.61	15.16	66.76	2.0259	1.862	.7994	2.31	34.53	98.88	5.1125	5.051	-.7894
1.62	15.45	67.33	2.0521	1.893	.7909	2.32	34.78	99.25	5.1813	5.114	-.8326
1.63	15.75	67.91	2.0786	1.926	.7818	2.33	35.03	99.61	5.2521	5.179	-.8766
1.64	16.04	68.47	2.1053	1.958	.7726	2.34	35.28	99.98	5.3220	5.242	-.9223
1.65	16.34	69.03	2.1313	1.990	.7628	2.35	35.53	100.35	5.3937	5.306	-.9692
1.66	16.63	69.59	2.1594	2.024	.7530	2.36	35.77	100.70	5.4675	5.372	-1.015
1.67	16.93	70.15	2.1872	2.057	.7428	2.37	36.02	101.06	5.5432	5.440	-1.063
1.68	17.22	70.69	2.2158	2.091	.7328	2.38	36.26	101.41	5.6148	5.504	-1.111
1.69	17.52	71.24	2.2452	2.126	.7221	2.39	36.50	101.77	5.6925	5.573	-1.161
1.70	17.81	71.78	2.2748	2.162	.7113	2.40	36.75	102.13	5.7703	5.642	-1.212
1.71	18.10	72.31	2.3031	2.194	.6999	2.41	36.99	102.47	5.8445	5.707	-1.262
1.72	18.40	72.85	2.3332	2.229	.6881	2.42	37.23	102.82	5.9242	5.777	-1.315
1.73	18.69	73.38	2.3641	2.265	.6761	2.43	37.47	103.17	6.0024	5.845	-1.367
1.74	18.98	73.90	2.3958	2.302	.6644	2.44	37.71	103.52	6.0864	5.918	-1.423
1.75	19.27	74.42	2.4254	2.336	.6515	2.45	37.95	103.88	6.1690	5.989	-1.478
1.76	19.58	74.94	2.4582	2.374	.6386	2.46	38.18	104.19	6.2461	6.056	-1.531
1.77	19.86	75.46	2.4907	2.411	.6254	2.47	38.42	104.54	6.3331	6.130	-1.590
1.78	20.15	75.97	2.5238	2.448	.6118	2.48	38.66	104.88	6.4193	6.204	-1.648
1.79	20.44	76.48	2.5562	2.485	.5976	2.49	38.89	105.21	6.5062	6.278	-1.707
1.80	20.73	76.98	2.5907	2.524	.5837	2.50	39.12	105.54	6.5920	6.351	-1.766
1.81	21.01	77.47	2.6239	2.561	.5693	2.51	39.36	105.88	6.6800	6.425	-1.828
1.82	21.30	77.97	2.6588	2.600	.5542	2.52	39.59	106.21	6.7659	6.497	-1.889
1.83	21.59	78.47	2.6947	2.640	.5387	2.53	39.82	106.54	6.8634	6.579	-1.954
1.84	21.88	78.96	2.7293	2.679	.5227	2.54	40.05	106.87	6.9541	6.655	-2.018
1.85	22.16	79.44	2.7663	2.720	.5071	2.55	40.28	107.19	7.0472	6.732	-2.082
1.86	22.45	79.93	2.8019	2.759	.4901	2.56	40.51	107.52	7.1429	6.811	-2.150
1.87	22.73	80.40	2.8409	2.801	.4736	2.57	40.75	107.84	7.2369	6.889	-2.217
1.88	23.02	80.89	2.8783	2.841	.4555	2.58	40.96	108.15	7.3298	6.965	-2.283
1.89	23.30	81.36	2.9163	2.883	.4380	2.59	41.19	108.48	7.4294	7.046	-2.355
1.90	23.59	81.83	2.9551	2.925	.4199	2.60	41.41	108.79	7.5301	7.129	-2.425

TABLE II. - Concluded. TWO-DIMENSIONAL FLOW AROUND CORNERS

| M	v	φ	$\frac{r}{r_0}$	$\frac{x}{r_0}$	$\frac{y}{r_0}$	M	v	φ	$\frac{r}{r_0}$	$\frac{x}{r_0}$	$\frac{y}{r_0}$
2.60	41.41	108.79	7.5301	7.129	-2.425	3.30	55.22	127.58	18.574	14.72	-11.33
2.61	41.64	109.11	7.6278	7.208	-2.497	3.31	55.39	127.81	18.811	14.86	-11.53
2.62	41.86	109.42	7.7280	7.288	-2.570	3.32	55.56	128.03	19.033	14.99	-11.73
2.63	42.09	109.74	7.8308	7.370	-2.645	3.33	55.73	128.25	19.279	15.14	-11.94
2.64	42.31	110.05	7.9428	7.461	-2.723	3.34	55.90	128.48	19.524	15.28	-12.15
2.65	42.53	110.36	8.0515	7.548	-2.801	3.35	56.07	128.70	19.755	15.42	-12.35
2.66	42.75	110.67	8.1500	7.625	-2.877	3.36	56.24	128.93	20.012	15.57	-12.58
2.67	42.97	110.97	8.2645	7.717	-2.958	3.37	56.41	129.15	20.272	15.72	-12.80
2.68	43.19	111.28	8.3682	7.797	-3.037	3.38	56.58	129.37	20.513	15.86	-13.01
2.69	43.40	111.58	8.4890	7.894	-3.122	3.39	56.75	129.59	20.781	16.01	-13.24
2.70	43.62	111.88	8.5985	7.979	-3.205	3.40	56.91	129.81	21.030	16.16	-13.46
2.71	43.84	112.19	8.7108	8.065	-3.290	3.41	57.07	130.02	21.286	16.30	-13.69
2.72	44.05	112.48	8.8183	8.148	-3.372	3.42	57.24	130.24	21.561	16.46	-13.93
2.73	44.27	112.78	8.9445	8.247	-3.463	3.43	57.40	130.45	21.784	16.58	-14.13
2.74	44.48	113.07	9.0580	8.333	-3.550	3.44	27.56	130.66	22.085	16.75	-14.39
2.75	44.69	113.37	9.1743	8.422	-3.639	3.45	57.73	130.88	22.361	16.91	-14.64
2.76	44.91	113.67	9.3023	8.520	-3.735	3.46	57.89	131.09	22.833	17.06	-14.88
2.77	45.12	113.96	9.4251	8.613	-3.828	3.47	58.05	131.30	22.909	17.21	-15.12
2.78	45.33	114.25	9.5511	8.709	-3.923	3.48	58.21	131.51	23.191	17.37	-15.37
2.79	45.54	114.54	9.6749	8.801	-4.018	3.49	58.37	131.72	23.477	17.52	-15.62
2.80	45.75	114.83	9.8039	8.898	-4.117	3.50	58.53	131.93	23.759	17.68	-15.88
2.81	45.95	115.10	9.9305	8.993	-4.213	3.51	58.69	132.14	24.056	17.84	-16.14
2.82	46.16	115.39	10.060	9.088	-4.314	3.52	58.85	132.35	24.372	18.01	-16.42
2.83	46.37	115.68	10.195	9.188	-4.417	3.53	59.00	132.54	24.643	18.16	-16.66
2.84	46.57	115.95	10.324	9.283	-4.518	3.54	59.16	132.75	24.950	18.32	-16.94
2.85	46.78	116.24	10.460	9.383	-4.624	3.55	59.32	132.96	25.259	18.48	-17.21
2.86	46.98	116.51	10.592	9.479	-4.728	3.56	59.47	133.16	25.569	18.65	-17.49
2.87	47.19	116.80	10.743	9.589	-4.844	3.57	59.63	133.36	25.867	18.81	-17.76
2.88	47.39	117.07	10.879	9.688	-4.951	3.58	59.78	133.56	26.185	18.98	-18.04
2.89	47.59	117.35	11.024	9.792	-5.064	3.59	59.94	133.77	26.511	19.14	-18.34
2.90	47.79	117.62	11.164	9.891	-5.176	3.60	60.09	133.96	26.788	19.28	-18.60
2.91	47.99	117.89	11.306	9.993	-5.289	3.61	60.24	134.16	27.152	19.48	-18.92
2.92	48.19	118.16	11.459	10.10	-5.408	3.62	60.40	134.36	27.473	19.64	-19.21
2.93	48.39	118.43	11.605	10.21	-5.525	3.63	60.55	134.56	27.816	19.82	-19.52
2.94	48.59	118.70	11.752	10.31	-5.643	3.64	60.70	134.75	28.137	19.98	-19.81
2.95	48.78	118.97	11.913	10.42	-5.771	3.65	60.85	134.95	28.490	20.16	-20.13
2.96	48.98	119.23	12.066	10.53	-5.892	3.66	61.00	135.14	28.818	20.33	-20.43
2.97	49.18	119.50	12.220	10.64	-6.017	3.67	61.15	135.34	29.155	20.49	-20.74
2.98	49.37	119.76	12.380	10.75	-6.145	3.68	61.30	135.53	29.525	20.68	-21.07
2.99	49.56	120.02	12.538	10.86	-6.273	3.69	61.45	135.73	29.878	20.85	-21.40
3.00	49.76	120.29	12.710	10.98	-6.411	3.70	61.60	135.92	30.221	21.02	-21.71
3.01	49.95	120.55	12.875	11.09	-6.544	3.71	61.74	136.10	30.581	21.20	-22.04
3.02	50.14	120.80	13.029	11.19	-6.672	3.72	61.89	136.30	30.969	21.40	-22.39
3.03	50.33	121.06	13.198	11.31	-6.809	3.73	62.04	136.49	31.338	21.58	-22.73
3.04	50.52	121.32	13.369	11.42	-6.949	3.74	62.18	136.67	31.691	21.75	-23.06
3.05	50.71	121.57	13.545	11.54	-7.091	3.75	62.33	136.86	32.082	21.94	-23.41
3.06	50.90	121.83	13.721	11.66	-7.236	3.76	62.47	137.05	32.457	22.12	-23.76
3.07	51.09	122.08	13.900	11.78	-7.382	3.77	62.61	137.23	32.841	22.30	-24.11
3.08	51.28	122.33	14.071	11.89	-7.525	3.78	62.76	137.42	33.234	22.49	-24.47
3.09	51.46	122.58	14.255	12.01	-7.676	3.79	62.90	137.60	33.591	22.65	-24.81
3.10	51.65	122.83	14.443	12.14	-7.831	3.80	63.04	137.78	33.990	22.84	-25.17
3.11	51.84	123.08	14.620	12.25	-7.980	3.81	63.19	137.97	34.400	23.03	-25.55
3.12	52.02	123.33	14.813	12.38	-8.140	3.82	63.33	138.15	34.819	23.23	-25.94
3.13	52.20	123.57	14.997	12.50	-8.293	3.83	63.47	138.33	35.236	23.42	-26.32
3.14	52.39	123.82	15.195	12.62	-8.458	3.84	63.61	138.52	35.651	23.62	-26.71
3.15	52.57	124.06	15.385	12.75	-8.617	3.85	63.75	138.70	36.088	23.82	-27.11
3.16	52.75	124.30	15.574	12.87	-8.776	3.86	63.89	138.88	36.483	23.99	-27.48
3.17	52.93	124.54	15.783	13.00	-8.949	3.87	64.03	139.05	36.928	24.20	-27.89
3.18	53.11	124.78	15.977	13.12	-9.113	3.88	64.16	139.22	37.327	24.38	-28.26
3.19	53.29	125.02	16.179	13.25	-9.285	3.89	64.30	139.40	37.751	24.57	-28.66
3.20	53.47	125.26	16.380	13.37	-9.456	3.90	64.44	139.58	38.197	24.77	-29.08
3.21	53.65	125.50	16.600	13.51	-9.640	3.91	64.58	139.76	38.625	24.95	-29.48
3.22	53.83	125.74	16.810	13.64	-9.819	3.92	64.71	139.93	39.093	25.16	-29.92
3.23	54.00	125.97	17.021	13.78	-10.00	3.93	64.85	140.11	39.573	25.38	-30.36
3.24	54.18	126.20	17.235	19.91	-10.18	3.94	64.98	140.28	39.984	25.55	-30.76
3.25	54.35	126.43	17.452	14.04	-10.36	3.95	65.12	140.46	40.519	25.79	-31.25
3.26	54.53	126.67	17.674	14.18	-10.55	3.96	65.25	140.62	40.917	25.96	-31.63
3.27	54.71	126.90	17.899	14.31	-10.75	3.97	65.39	140.80	41.425	26.18	-32.10
3.28	54.88	127.13	18.126	14.45	-10.94	3.98	65.52	140.97	41.929	26.40	-32.57
3.29	55.05	127.35	18.339	14.58	-11.13	3.99	65.65	141.14	42.409	26.61	-33.02
3.30	55.22	127.58	18.574	14.72	-11.33·	4.00	65.78	141.30	42.844	26.79	-33.44
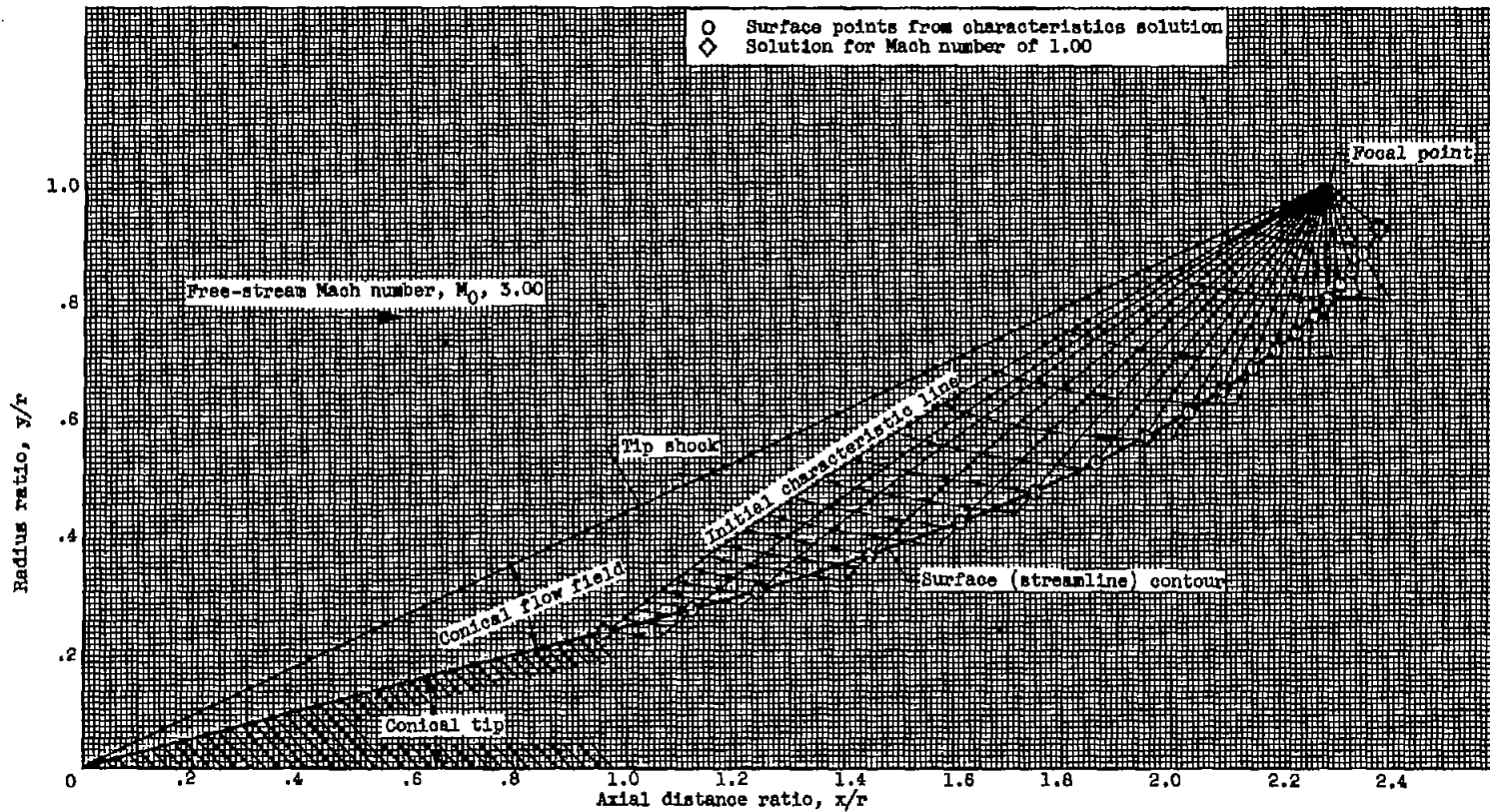
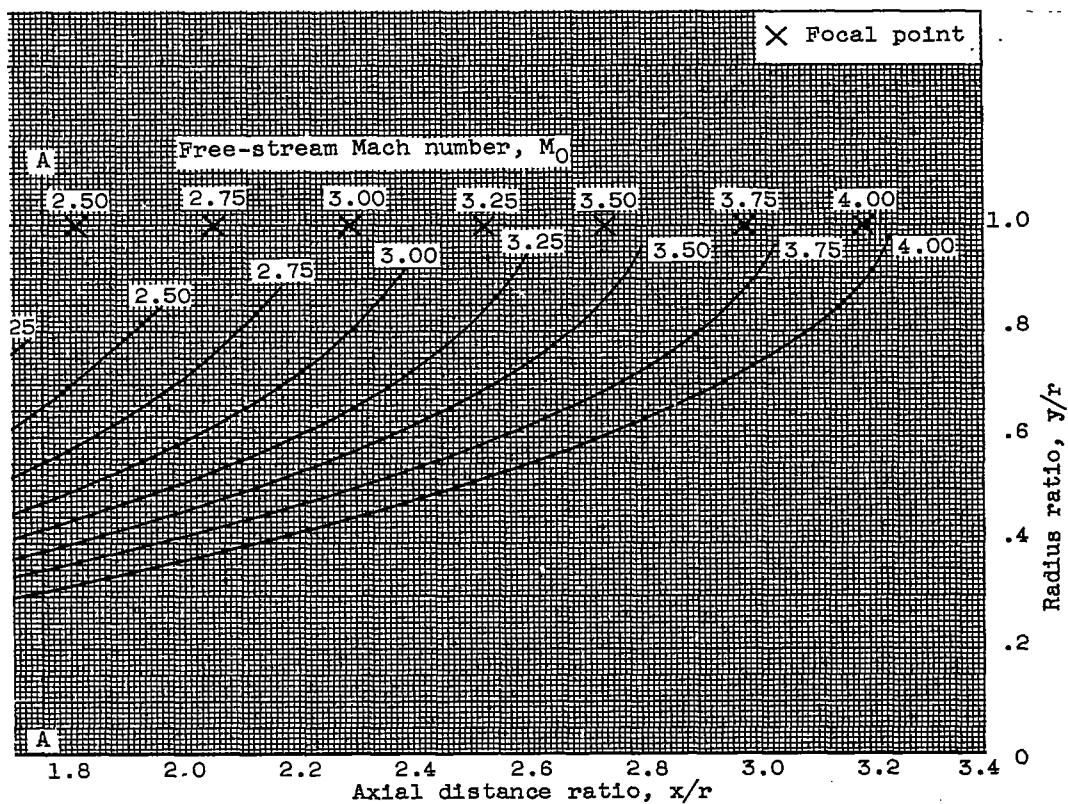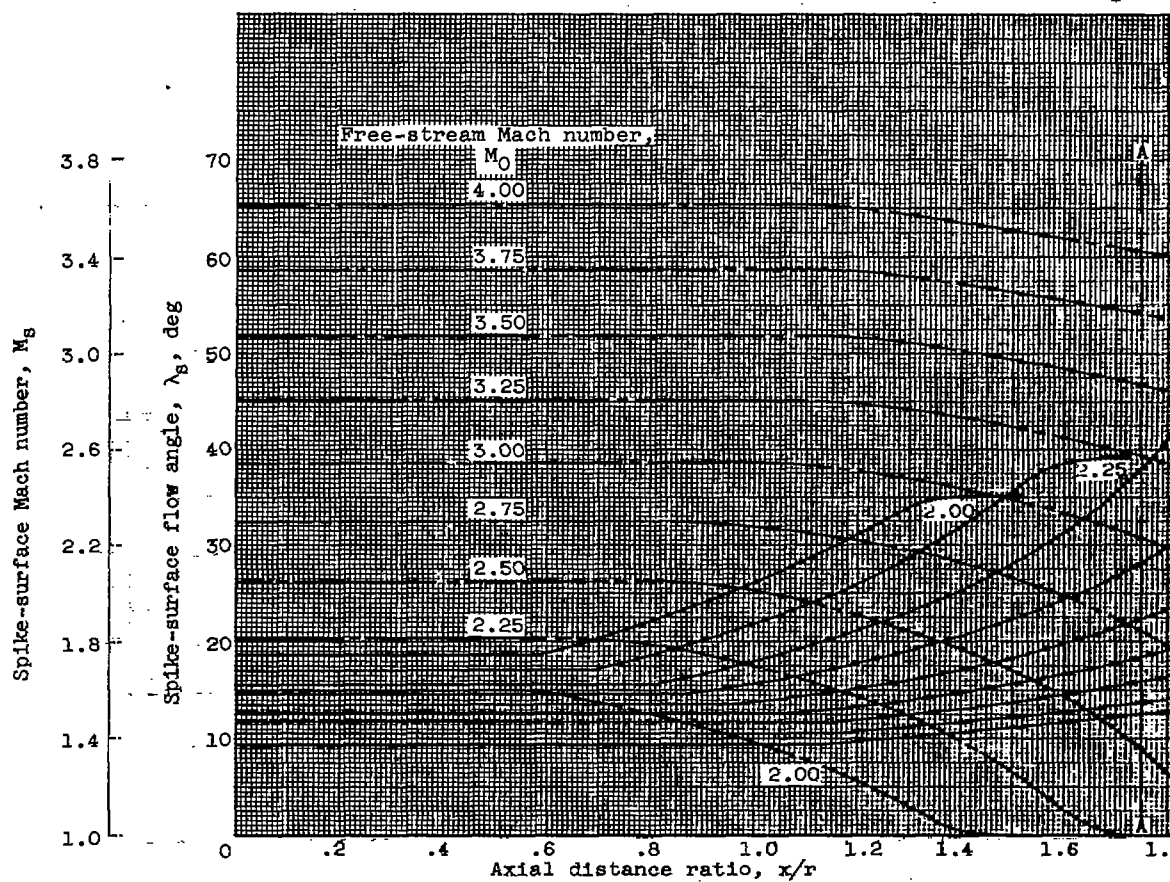Figure 1. - Typical axisymmetric characteristics solution for isentropic spike.
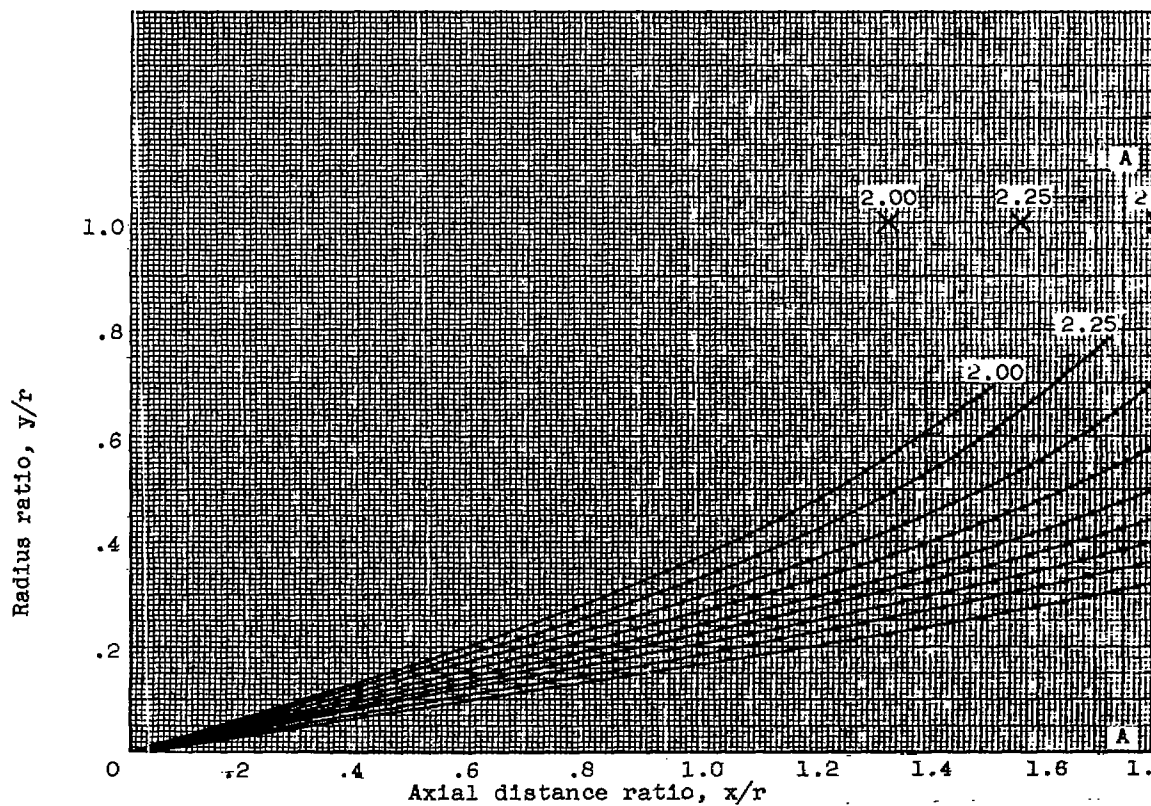
(a) Geometric contours.

Figure 2. - Aerodynamic design parameters for isentropic axisym-
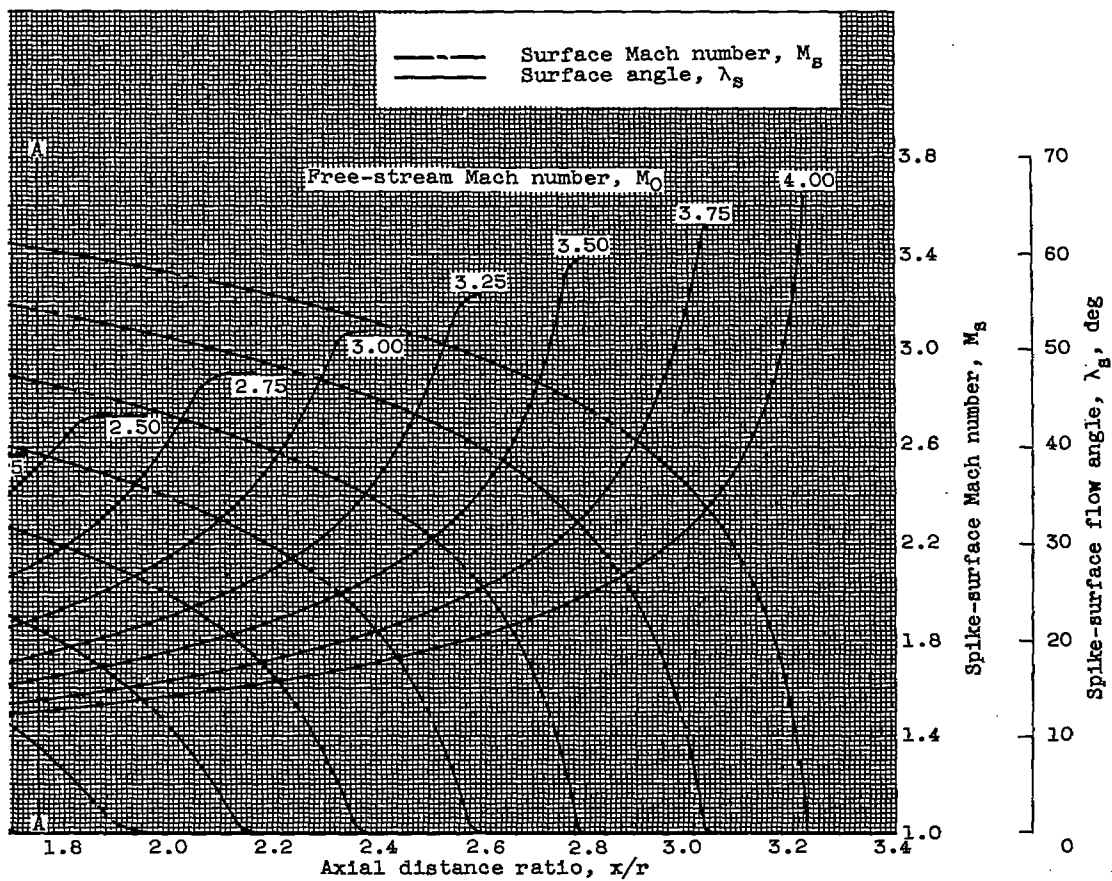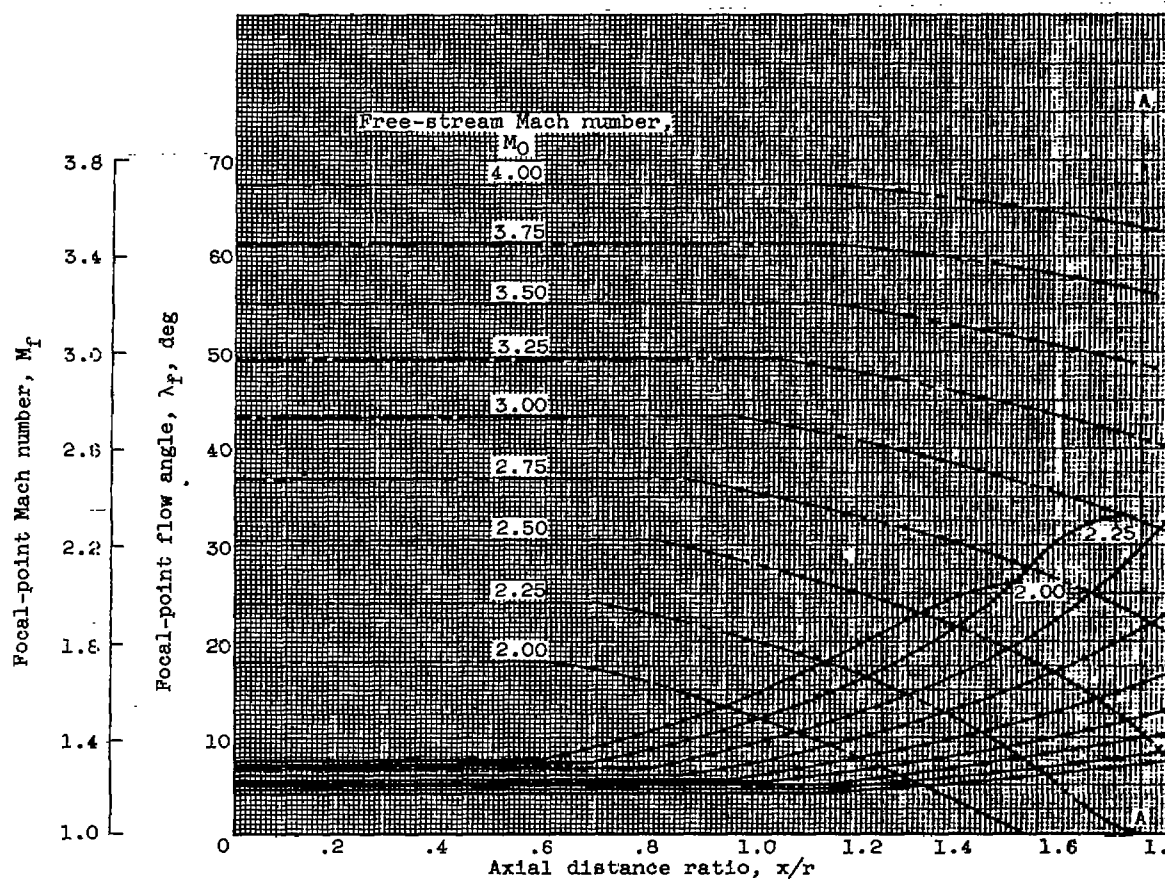metric spikes.

3659

CS-3 back

X Focal point

Free-stream Mach number, M_0

A

| 2.50 | 2.75 | 3.00 | 3.25 | 3.50 | 3.75 | 4.00 |

2.75   3.00   3.25   3.50   3.75   4.00

2.50

1.0

.8

.6

.4

.2

0

A

Radius ratio, y/r

1.8   2.0   2.2   2.4   2.6   2.8   3.0   3.2   3.4
Axial distance ratio, x/r

(b) Surface flow angle and Mach number.

Figure 2. - Continued.   Aerodynamic design parameters for isentropic
axisymmetric spikes.

3659

(c) Focal-point flow angle and Mach number.

Figure 2. - Concluded.   Aerodynamic design parameters for isentropic
   axisymmetric spikes

Axial distance ratio, x/r

Focal-point Mach number, M_f

Focal-point flow angle, λ_f, deg
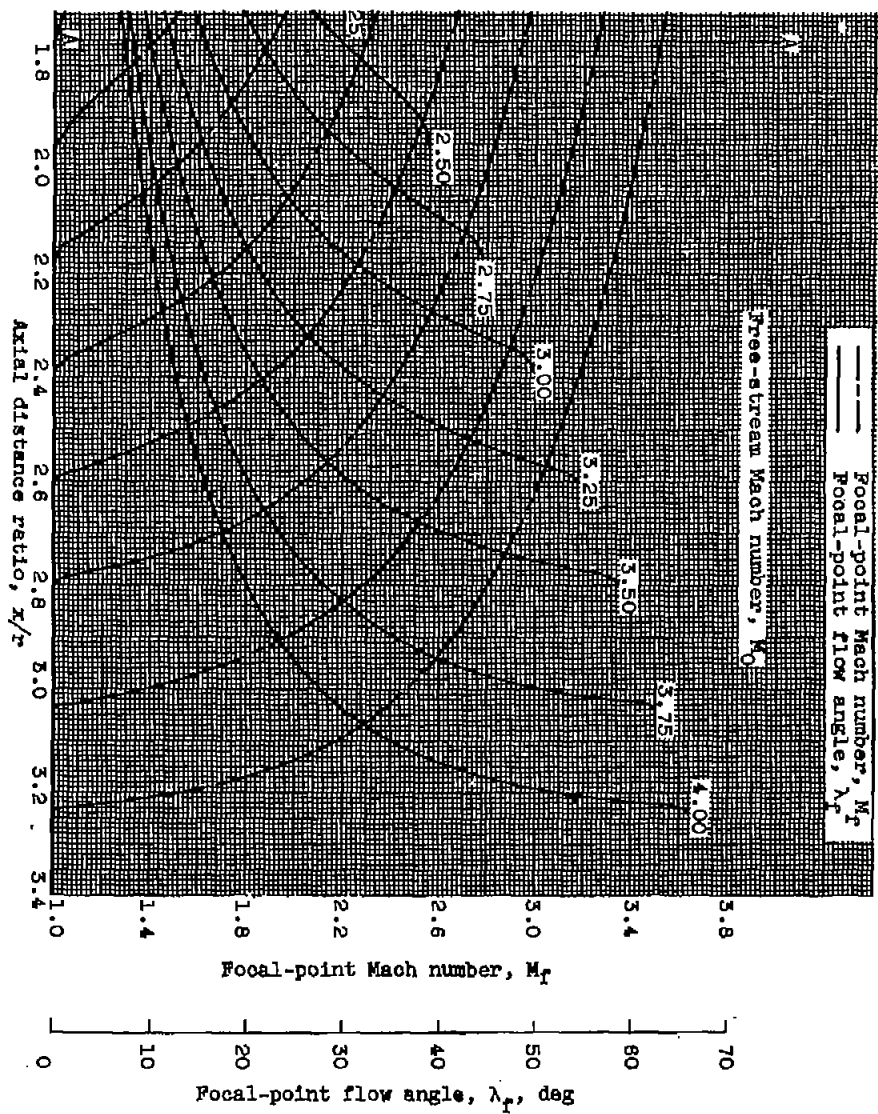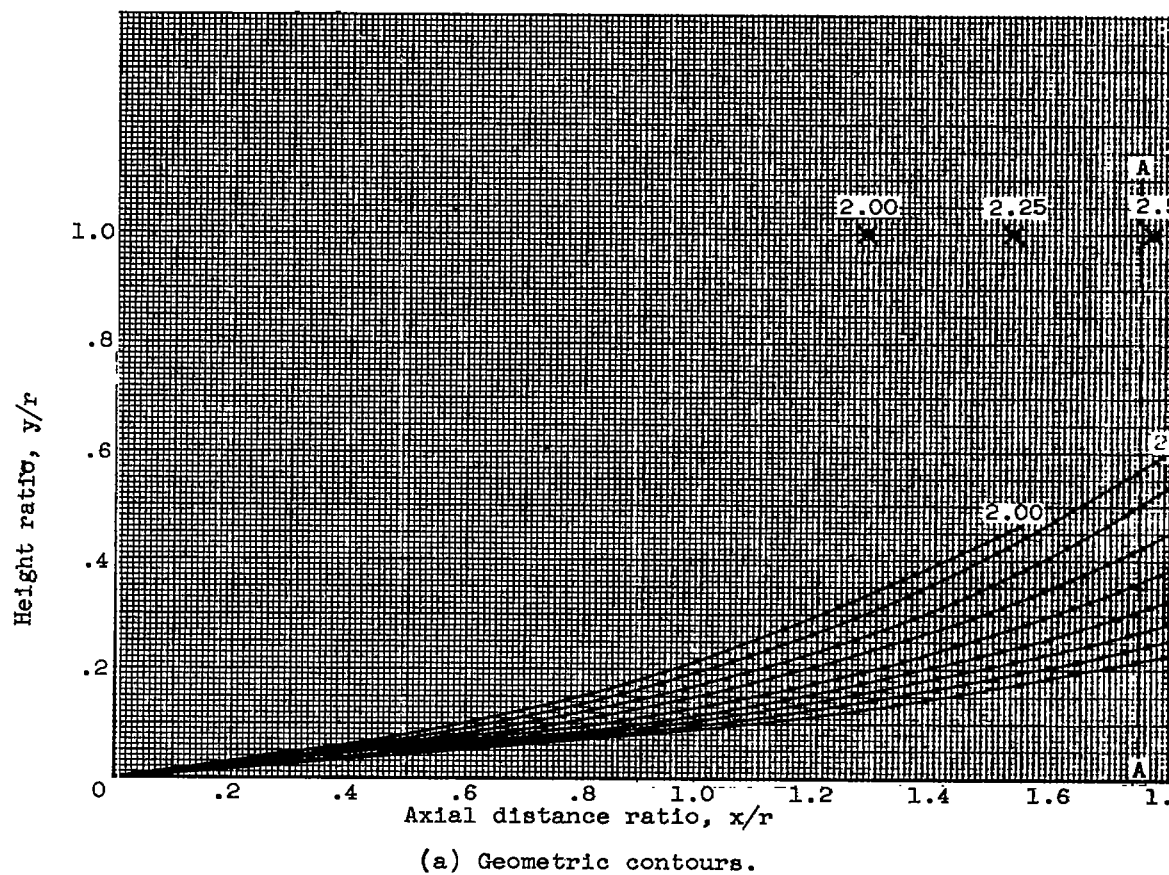
(a) Geometric contours.

Figure 3. - Aerodynamic design parameters for isentropic two-dimensional ramps.
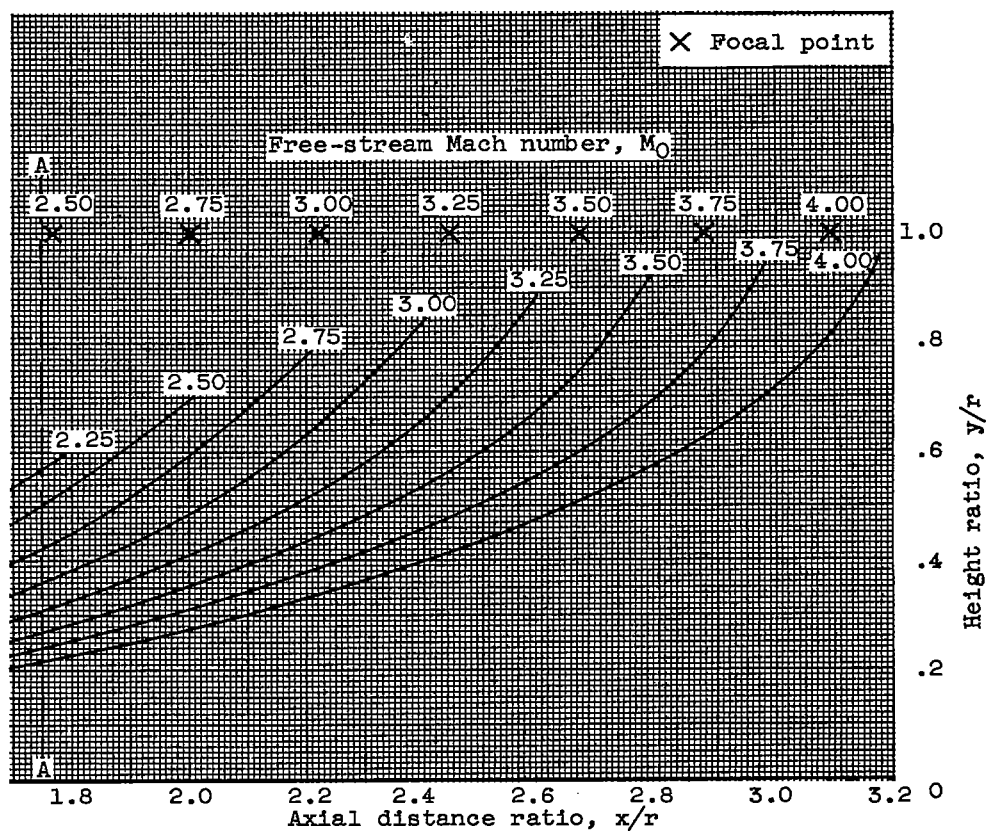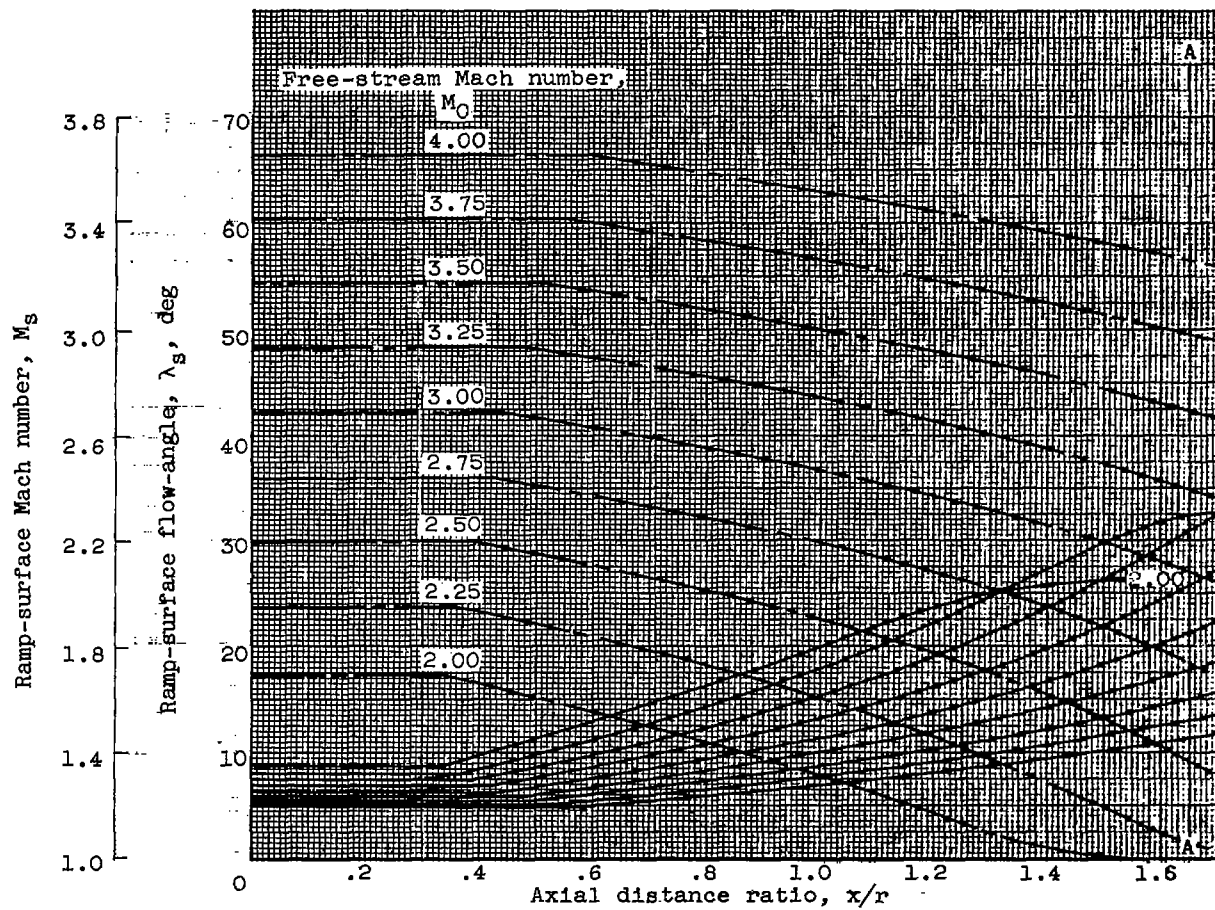
(b) Mach number and flow-angle variation.

Figure 3. - Concluded. Aerodynamic design parameters for isentropic
two-dimensional ramps.

3659

CS-4 back
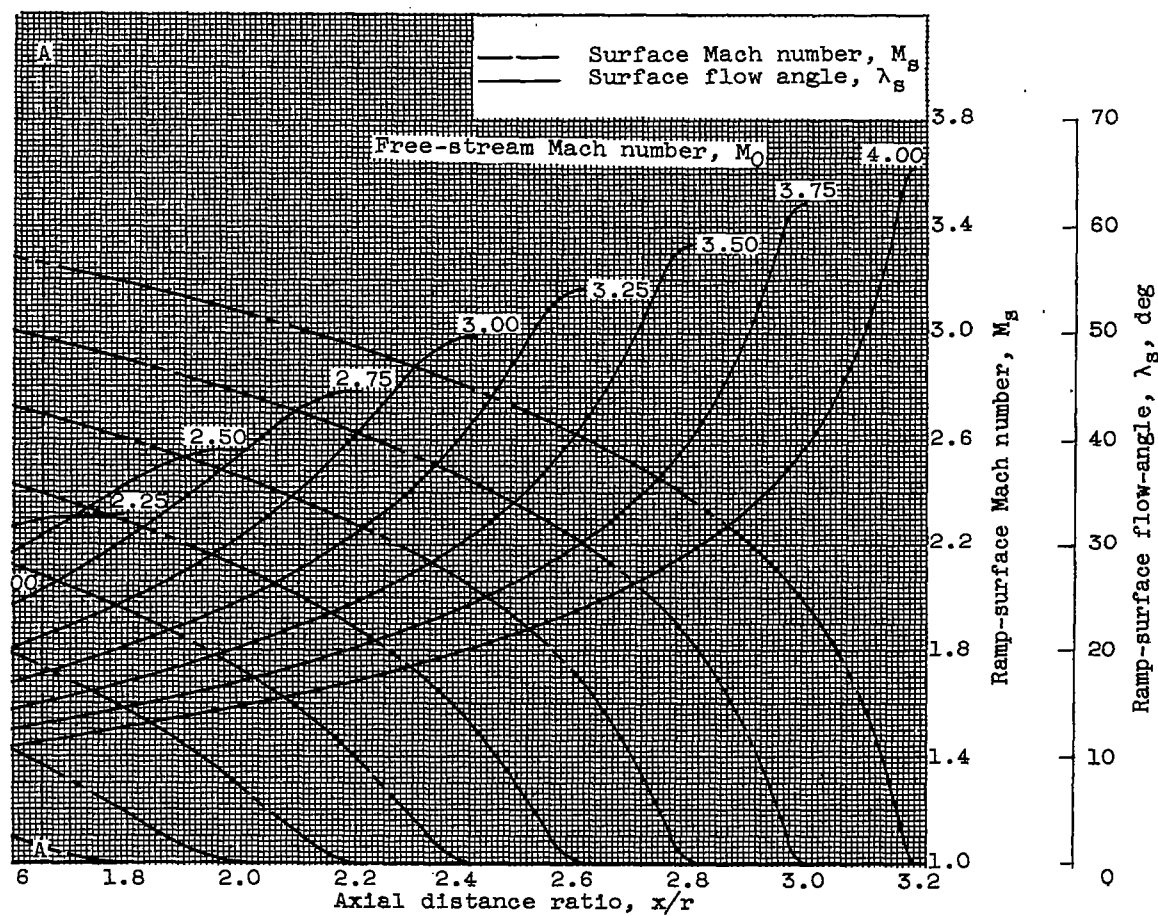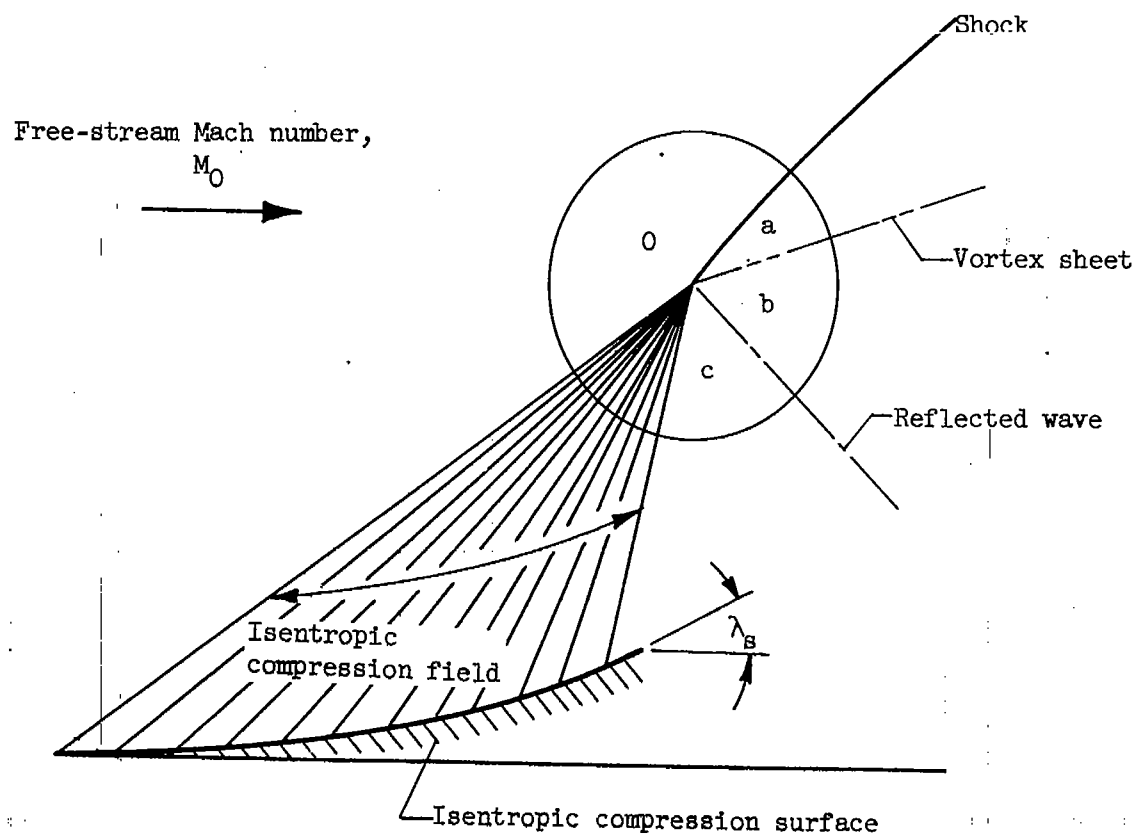
Figure 4. - Schematic representation of branch-shock structure to be analyzed for maximum isentropic flow turning.
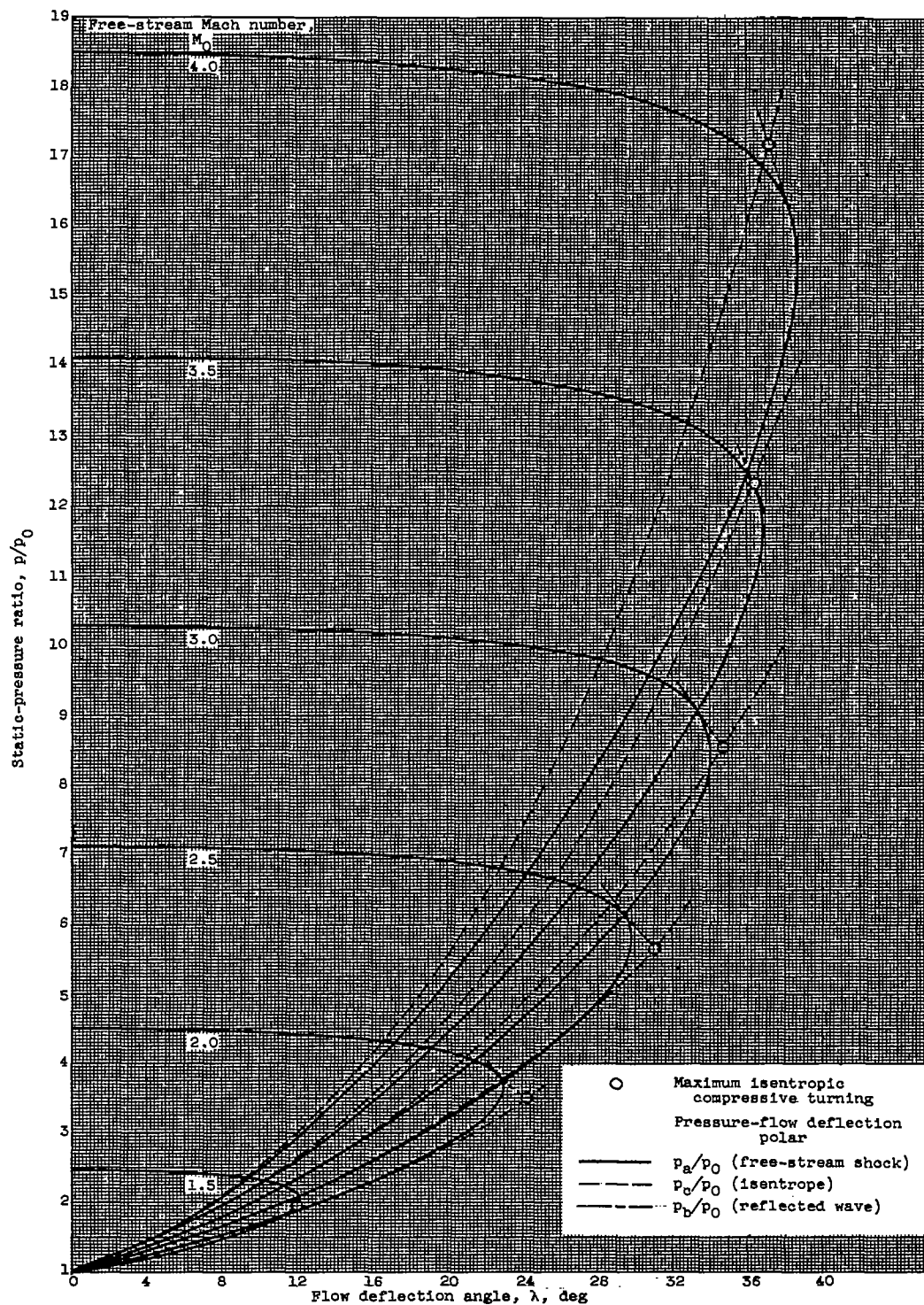
Figure 5. - Theoretical pressure-deflection polars.
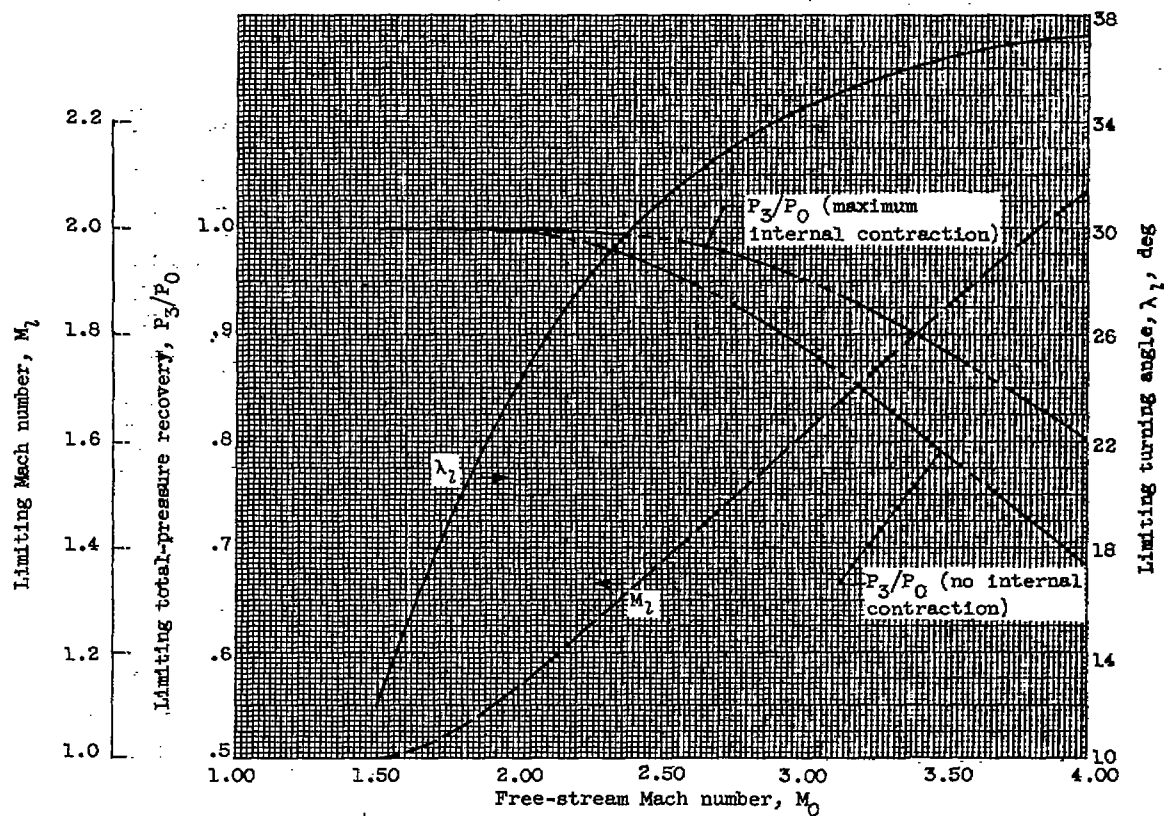
Figure 6. - Summary of aerodynamic parameters corresponding to compression
limit based on shock-structure requirements.
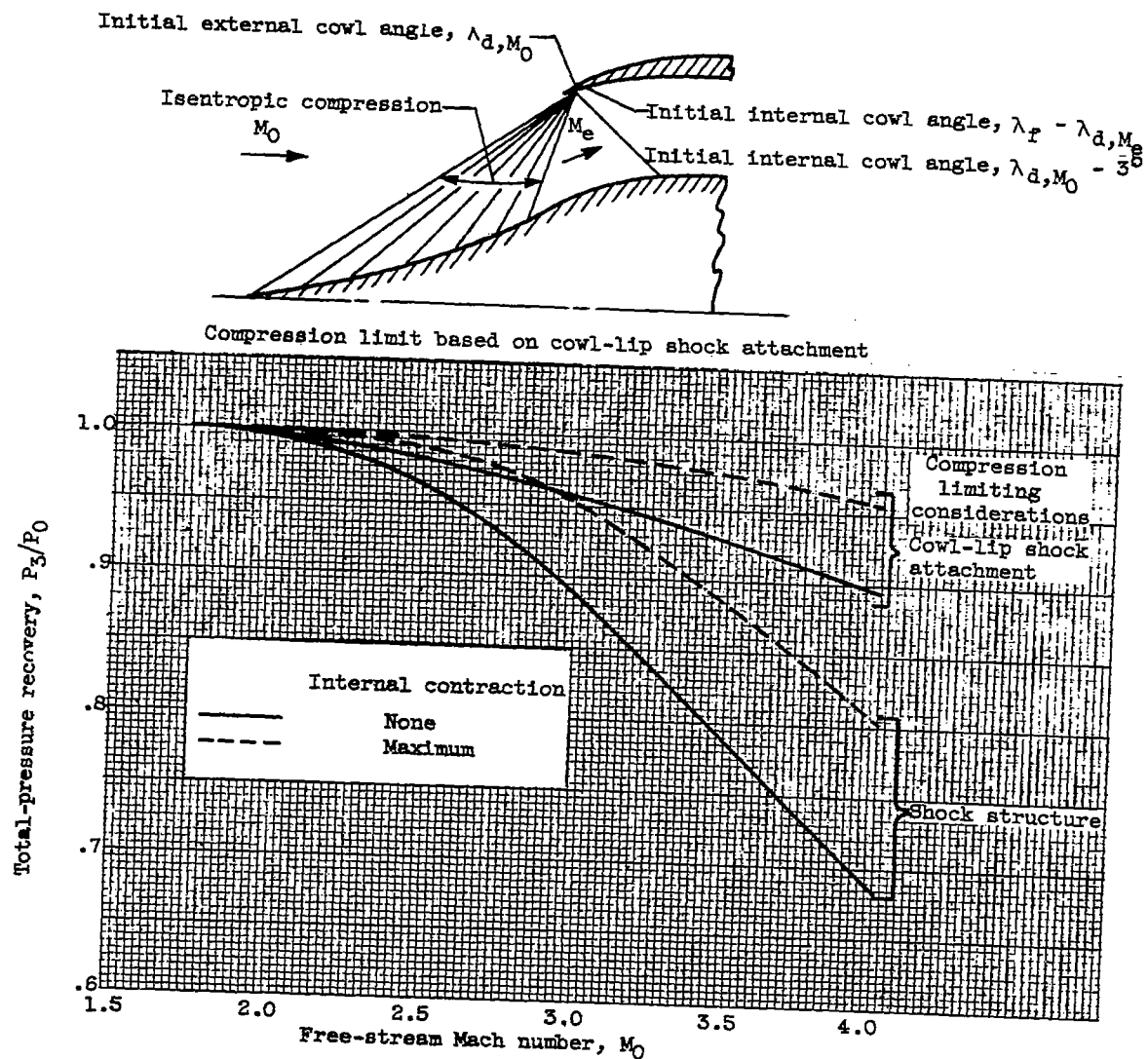
Figure 7. - Comparison of compression limits based on cowl-lip shock attachment and shock-structure considerations.
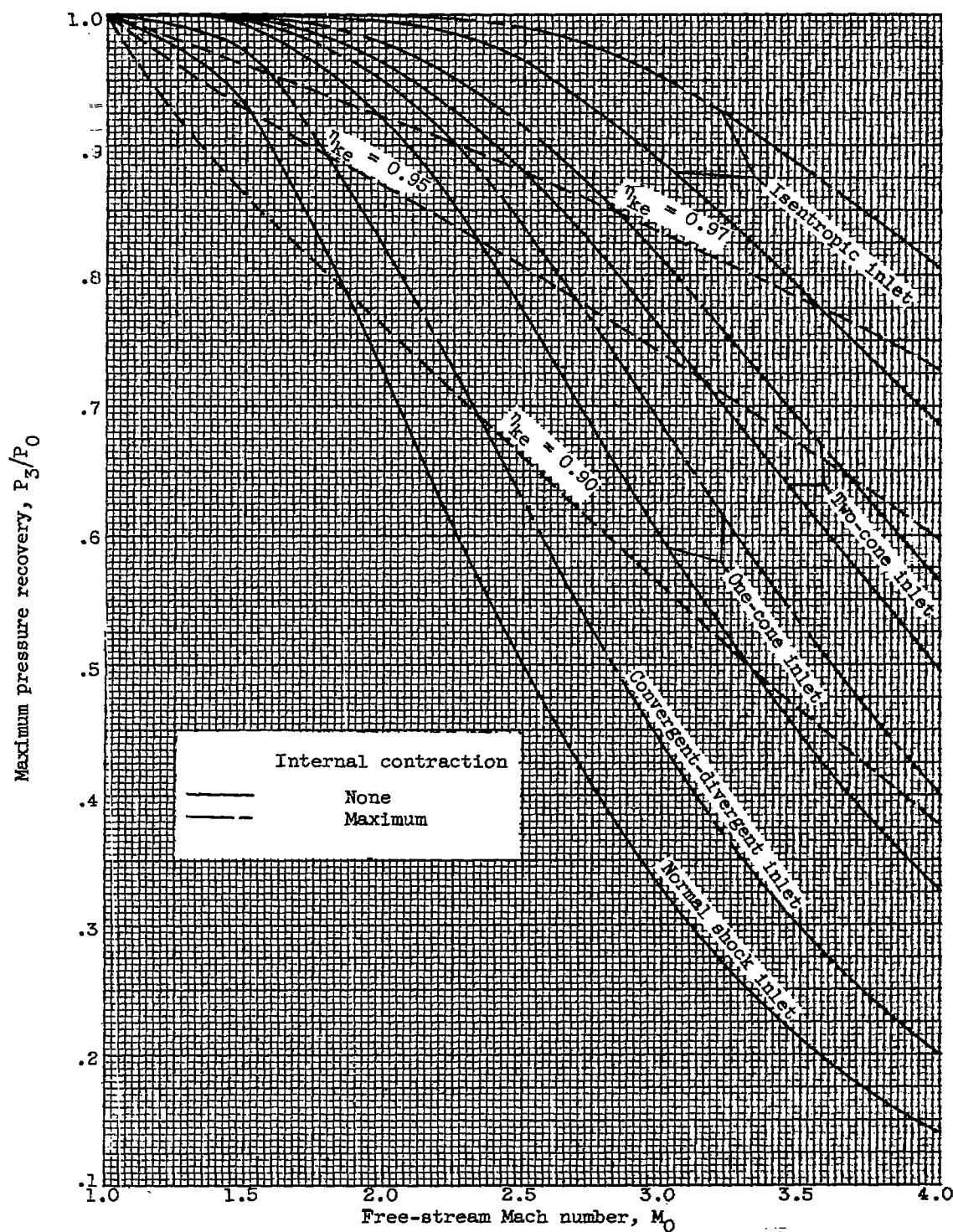
Figure 8. - Theoretical performance comparison of several types of supersonic inlets.
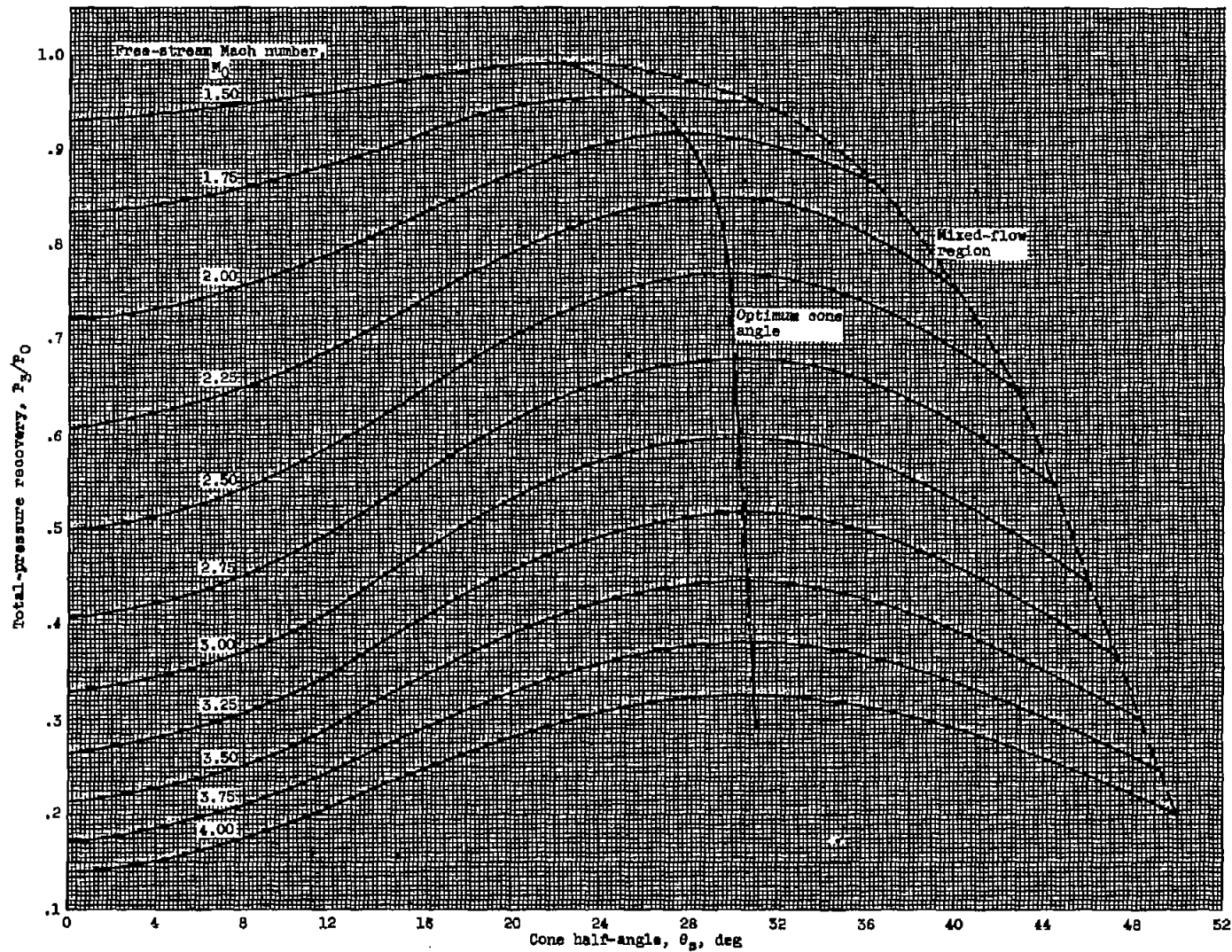
(a) Single-cone inlets; no internal contraction.

Figure 9. - Theoretical performance of single-cone and single-wedge inlets.
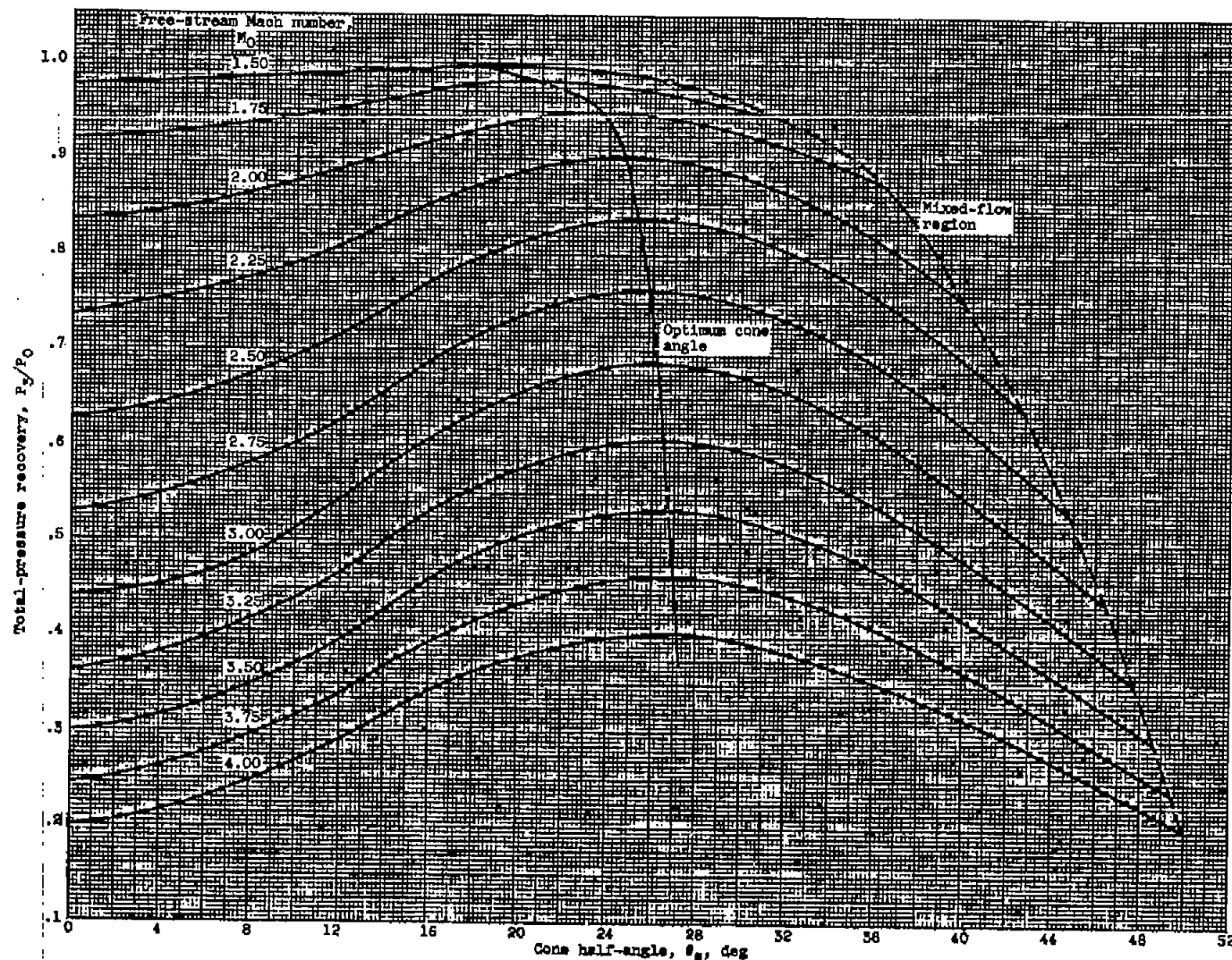
(b) Single-cone inlets; maximum allowable internal contraction.

Figure 9. — Continued. Theoretical performance of single-cone and single-wedge inlets.
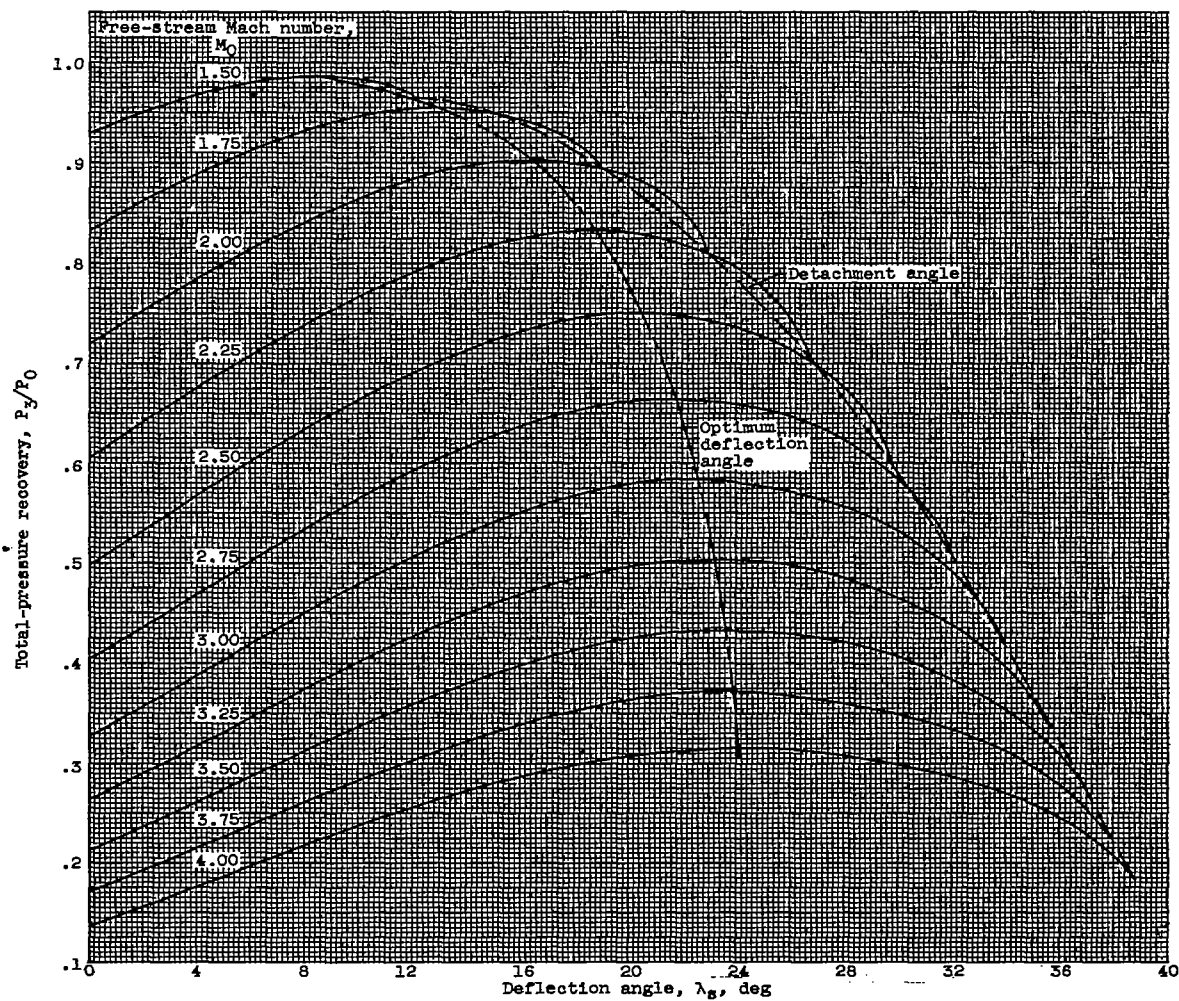
(c) Single-wedge inlets; no internal contraction.

Figure 9. – Continued. Theoretical performance of single-cone and single-wedge inlets.
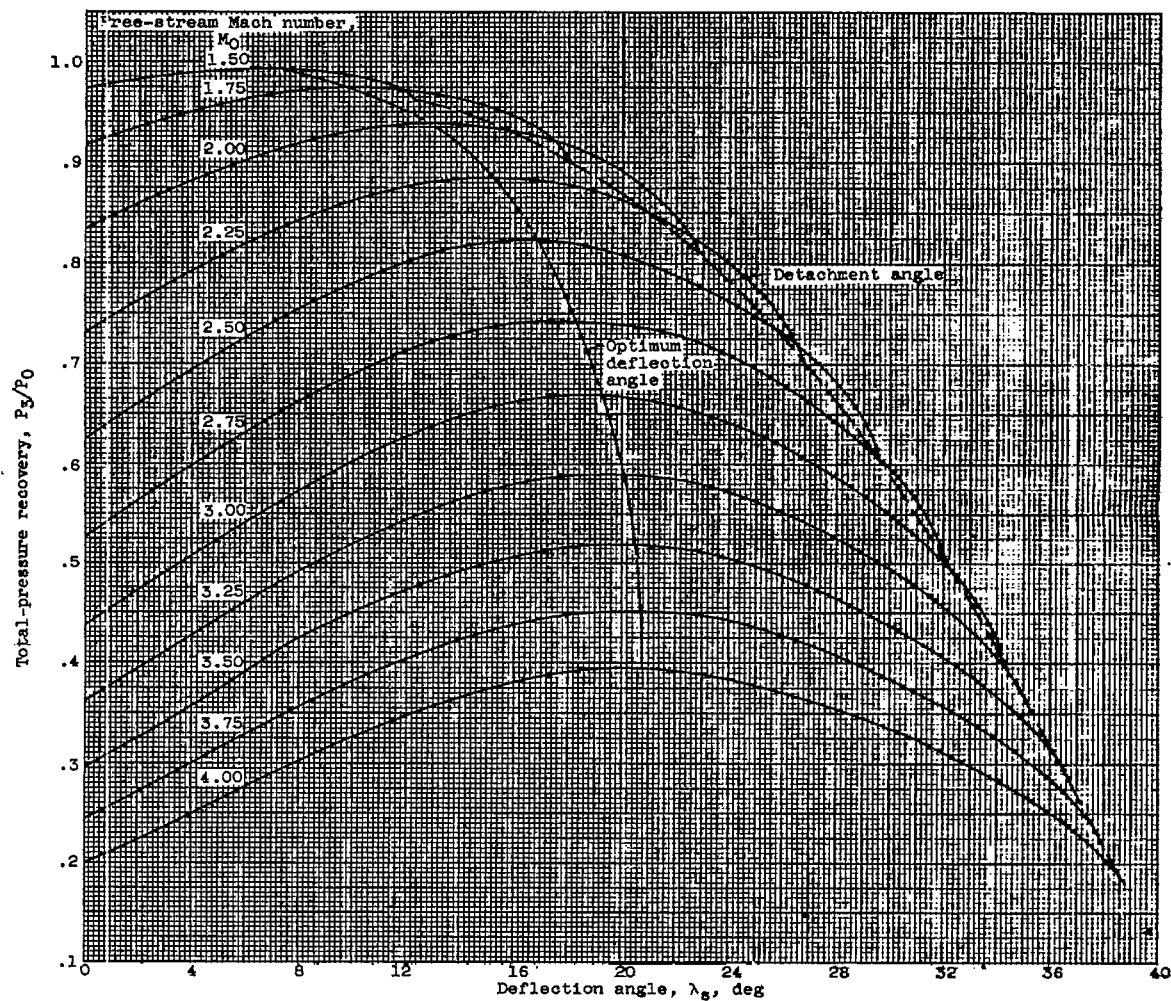
(d) Single-wedge inlets; maximum allowable internal contraction.

Figure 9. - Concluded.   Theoretical performance of single-cone and single-wedge inlets.
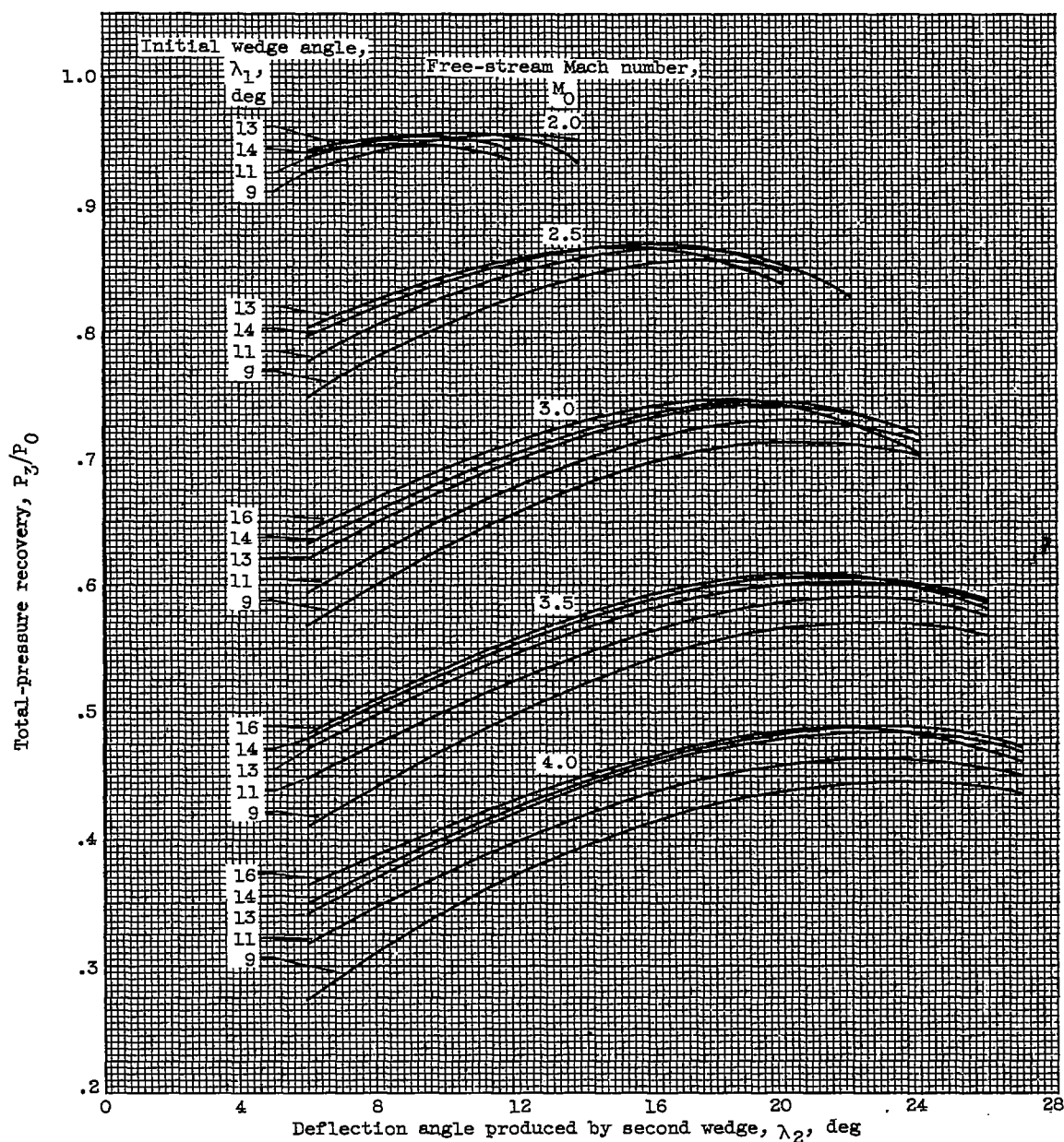
3659
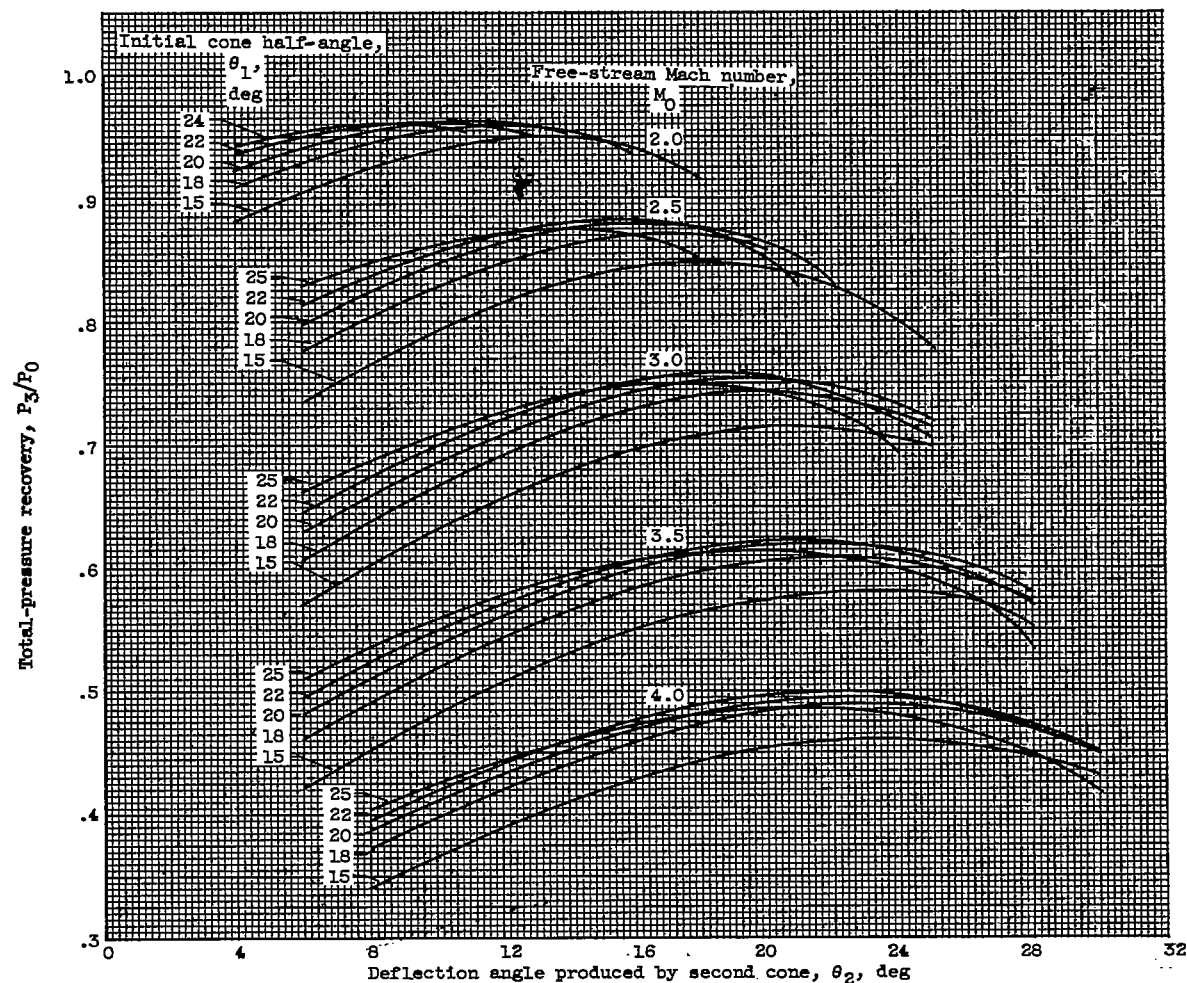
(a) Double-cone inlets; no internal contraction.

Figure 10. - Theoretical performance of double-cone and double-wedge inlets.
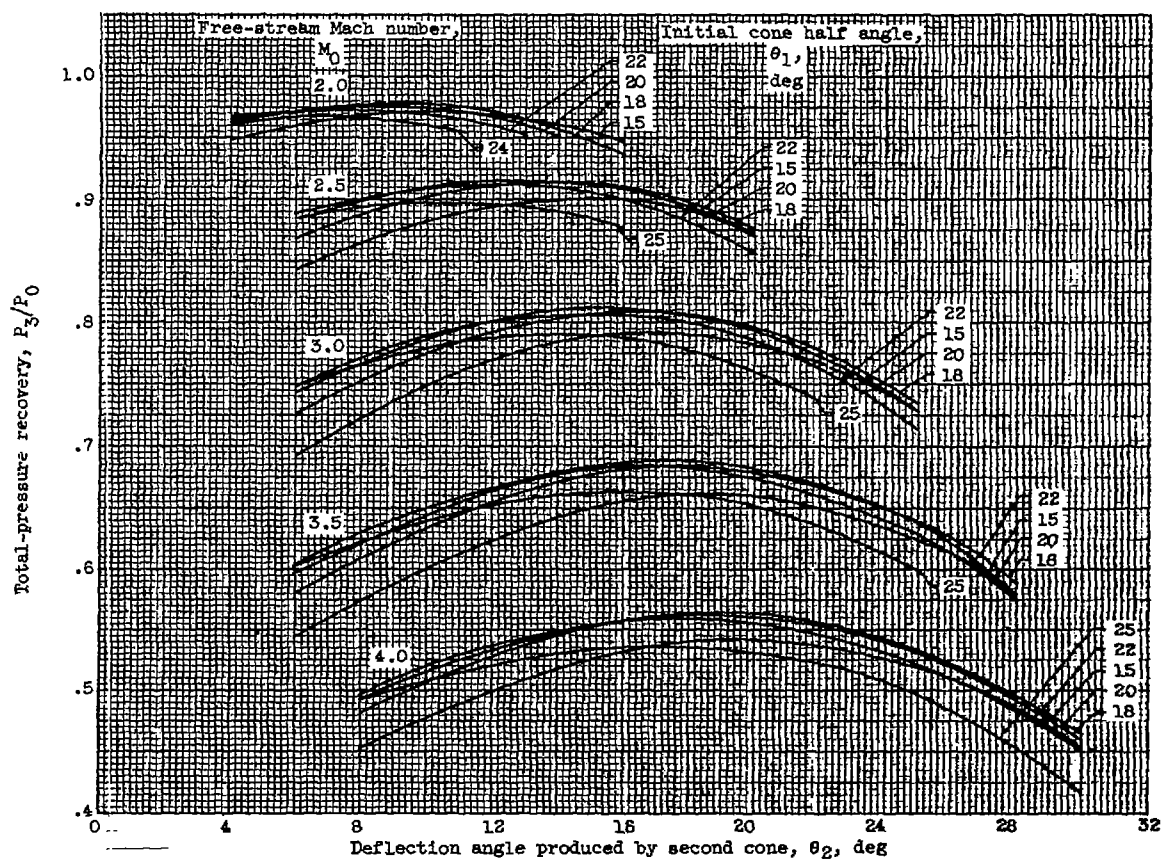
(b) Double-cone inlets; maximum allowable internal contraction.

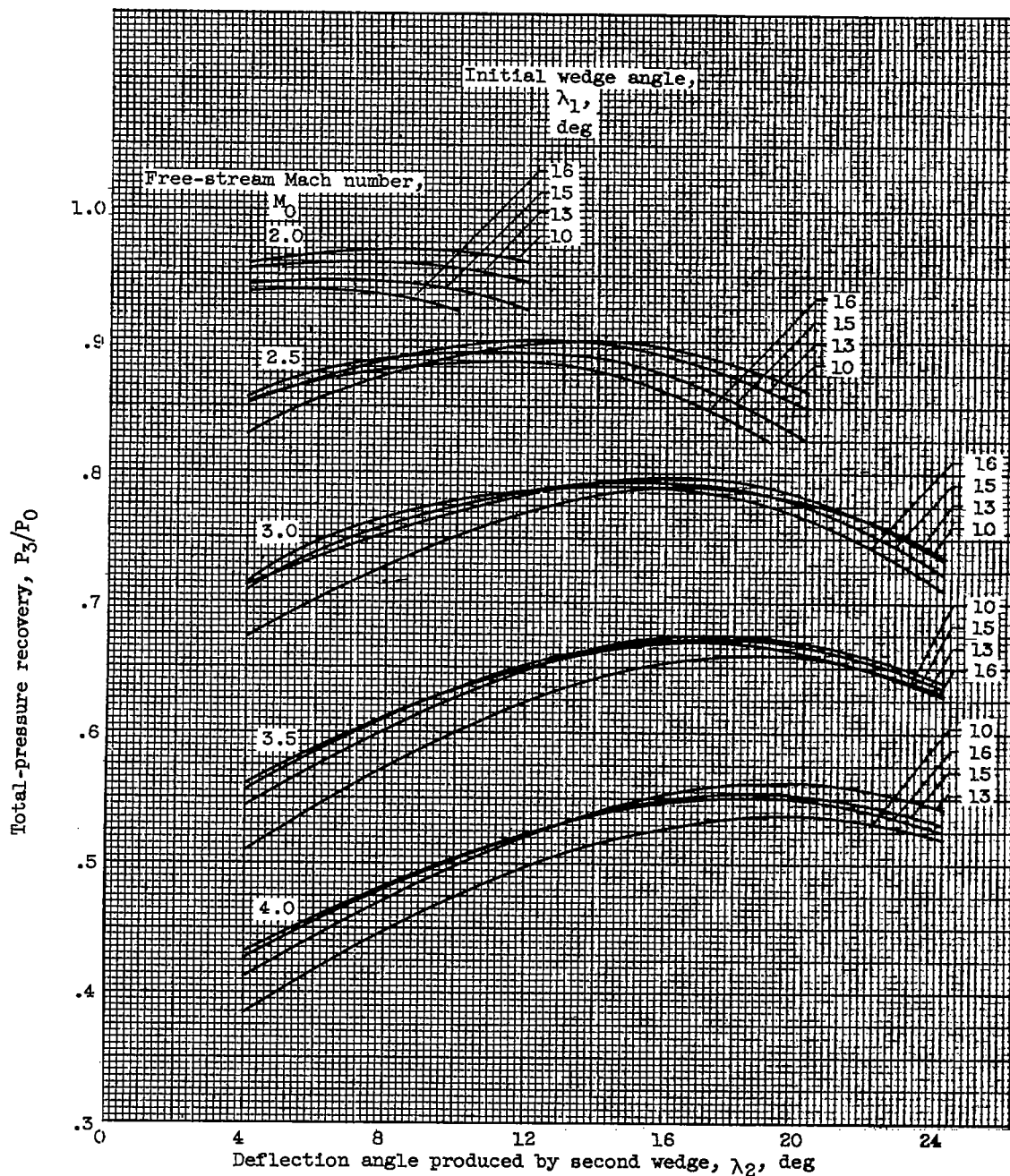Figure 10. - Continued. Theoretical performance of double-cone and double-wedge inlets.
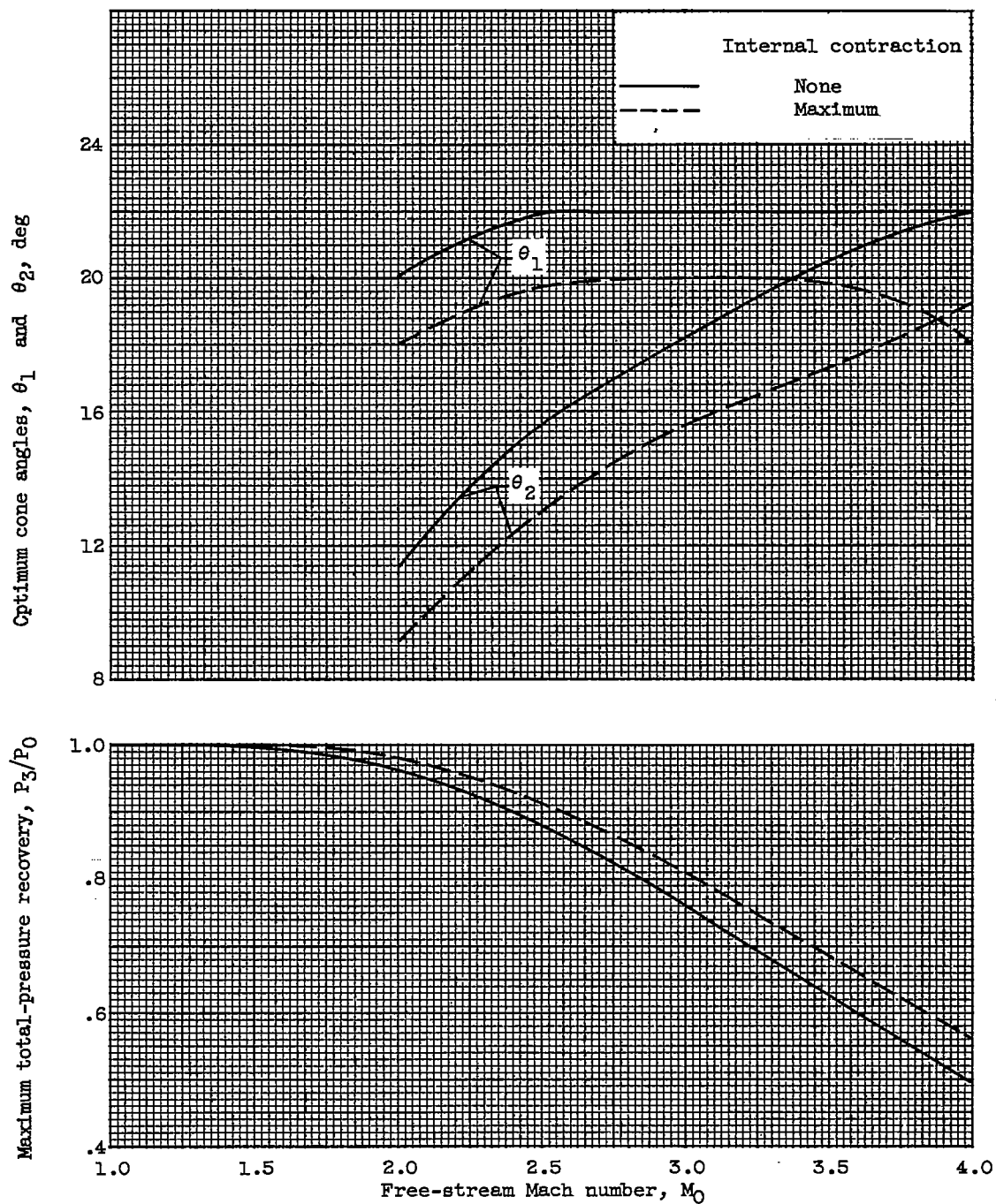
(c) Double-wedge inlets; no internal contraction.

Figure 10. - Continued. Theoretical performance of double-cone and double-wedge inlets.
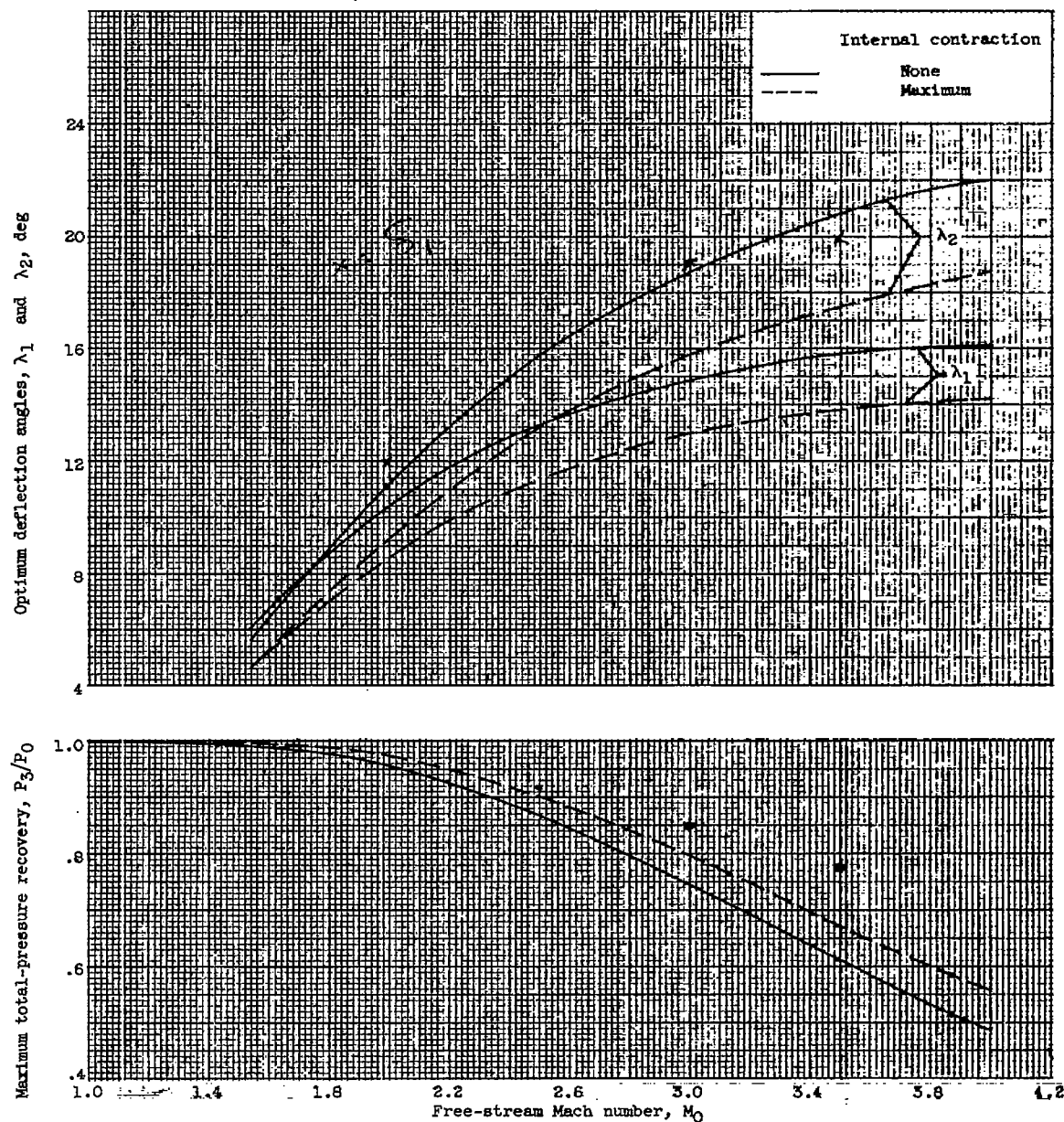
3659

(d) Double-wedge inlets; maximum allowable internal contraction.

Figure 10. - Concluded. Theoretical performance of double-cone and double-wedge inlets.

(a) Double-cone inlets.

Figure 11. - Optimum performance and angle combinations for double-oblique-shock supersonic inlets.

(b) Double-wedge inlets.

Figure 11. - Concluded. Optimum performance and angle combinations for double-oblique-shock super-
sonic inlets.